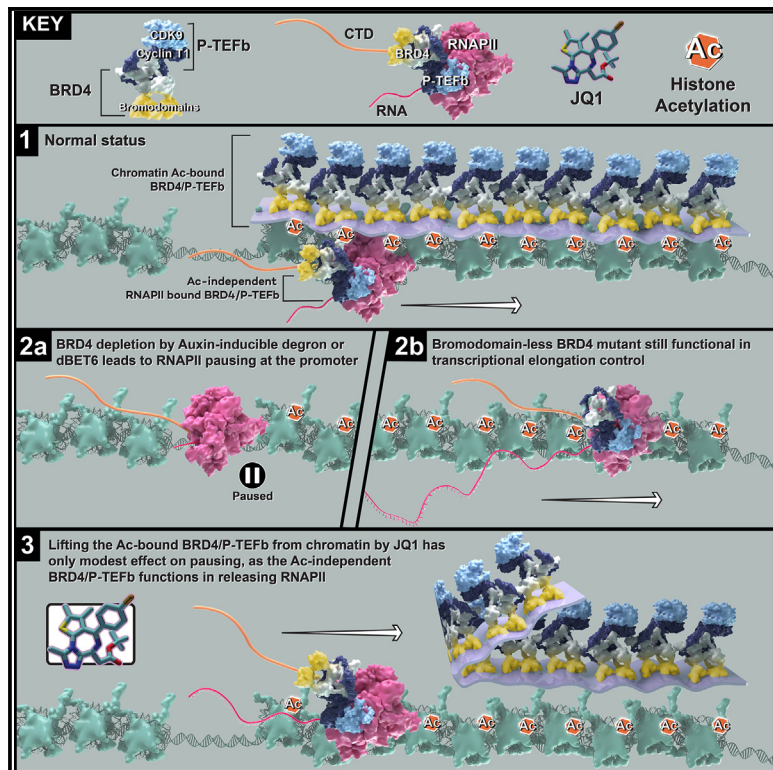


Distinct layers of BRD4-PTEFb reveal bromodomain-independent function in transcriptional regulation

Graphical abstract



Authors

Bin Zheng, Sarah Gold,
Marta Iwanaszko,
Benjamin Charles Howard, Lu Wang,
Ali Shilatifard

Correspondence

lu.wang1@northwestern.edu (L.W.),
ash@northwestern.edu (A.S.)

In brief

Zheng et al. demonstrate that while the regulation of Pol II pause release by BRD4 does not require bromodomain-mediated BRD4 binding to acetylated histones, a bromodomain-less, C-terminal fragment of BRD4 is both necessary and sufficient to drive the release of paused Pol II into productive elongation.

Highlights

- Unlike BETi (JQ1), BRD4 degradation causes profound Pol II pausing genome wide
- The bromodomains of BRD4 are dispensable for Pol II pause release in living cells
- A BET-less C-terminal BRD4 fragment interacts with PTEFb and releases paused Pol II
- The C-terminal disordered region of BRD4 secures cyclin T1 in the BRD4-PTEFb complex



Article

Distinct layers of BRD4-PTEFb reveal bromodomain-independent function in transcriptional regulation

Bin Zheng,¹ Sarah Gold,¹ Marta Iwanaszko,¹ Benjamin Charles Howard,¹ Lu Wang,^{1,*} and Ali Shilatifard^{1,2,*}

¹Simpson Querrey Institute for Epigenetics and the Department of Biochemistry and Molecular Genetics, Northwestern University Feinberg School of Medicine, Chicago, IL 60611, USA

²Lead contact

*Correspondence: lu.wang1@northwestern.edu (L.W.), ash@northwestern.edu (A.S.)

<https://doi.org/10.1016/j.molcel.2023.06.032>

SUMMARY

The BET family protein BRD4, which forms the CDK9-containing BRD4-PTEFb complex, is considered to be a master regulator of RNA polymerase II (Pol II) pause release. Because its tandem bromodomains interact with acetylated histone lysine residues, it has long been thought that BRD4 requires these bromodomains for its recruitment to chromatin and transcriptional regulatory function. Here, using rapid depletion and genetic complementation with domain deletion mutants, we demonstrate that BRD4 bromodomains are dispensable for Pol II pause release. A minimal, bromodomain-less C-terminal BRD4 fragment containing the PTEFb-interacting C-terminal motif (CTM) is instead both necessary and sufficient to mediate Pol II pause release in the absence of full-length BRD4. Although BRD4-PTEFb can associate with chromatin through acetyl recognition, our results indicate that a distinct, active BRD4-PTEFb population functions to regulate transcription independently of bromodomain-mediated chromatin association. These findings may enable more effective pharmaceutical modulation of BRD4-PTEFb activity.

INTRODUCTION

Transcription catalyzed by RNA polymerase II (Pol II) is tightly regulated at the distinct stages of initiation, pausing, elongation, and termination.^{1–3} Pol II promoter-proximal pausing is a prominent feature at the majority of the genes in human cells, and the positive transcription elongation factor (P-TEFb or PTEFb), which consists of the catalytic subunit CDK9 and the regulatory subunit cyclin T, is an essential complex that regulates the release of promoter-proximal-paused Pol II into elongation in gene bodies.^{4,5} Mechanistic studies have revealed that PTEFb mainly phosphorylates the serine residues at positions 2 and 5 of the heptapeptide repeats (52, in mammals) within the C-terminal domain (CTD) of RPB1, the main subunit of Pol II.^{6,7} PTEFb has also been shown to participate in multiple complexes, including the active BRD4-PTEFb complex, the active super elongation complex (SEC), and the inactive 7SK-HEXIM complex, in which a majority of PTEFb is sequestered.^{8–11} We previously demonstrated that PTEFb can be recruited to Pol II by either BRD4 under normal conditions or by the SEC under stress conditions such as heat shock.¹²

BRD4 is a member of the BET protein family, which also includes BRD2, BRD3, and BRDT. Each BET family member has two tandem bromodomains, which can bind with high affinity to acetylated lysines within histone tails, and an extraterminal (ET)

domain, which can interact with multiple transcription factors. However, only BRD4 and BRDT have C-terminal regions that can interact with PTEFb.^{13,14} Histone acetylation, especially the extensively studied H3K27ac, is a marker of active chromatin.^{15–17} Thus, a dominant model in the field holds that BRD4 bound to H3K27ac at promoters or enhancers recruits PTEFb to release paused Pol II, promoting transcription.^{18,19} In accordance with this model, bromodomain inhibitors have been developed and are now widely used both in research and in clinical trials; JQ1 is the most prominent example of a bromodomain inhibitor compound.²⁰ JQ1-based proteolysis targeting chimeras (PROTACs) such as dBET6 target bromodomain-containing proteins for degradation. However, the effects of PROTAC-induced BRD4 depletion differ strikingly from the effects of bromodomain inhibition.^{21–24} Some attempts to explain these differences focus on incomplete displacement of BRD4 from chromatin after JQ1 treatment. However, accumulating evidence calls in to question the assumed requirement for H3K27ac marks in transcriptional regulation.^{25–27} A recent study suggests that histone acetylation may not always be instructive to transcription, as complementation with catalytic-dead CBP or P300 mutants can restore gene expression just as well as their wild-type (WT), catalytic-active counterparts.²⁸ Therefore, in this study we aimed to test the established model by scrutinizing the functions of individual BRD4 domains using genetic complementation after acute depletion



of endogenous BRD4. These rescue experiments revealed that BRD4 participates in Pol II pause release independently of its bromodomains binding to acetylated histones. We tested this phenomenon in distinct human cell lines, gaining confidence in the broad mechanistic implication. A “layer” of BRD4-PTEFb is associated with chromatin through BRD4 bromodomain-mediated interactions with acetylated histones. However, our study reveals that when we remove this layer, either by disrupting the interaction of BRD4 bromodomains with acetylation or through replacement of endogenous BRD4 with bromodomain-less versions, Pol II pause release remains functional genome-wide. Our genetic and molecular studies have also resulted in the identification of a BRD4 region necessary for Pol II pause release that functions independently of any bromodomain-mediated chromatin association. Altogether, this study introduces an important and possibly singular mechanism of histone acetylation-independent transcriptional regulatory function for BRD4, providing a basis for specific pharmaceutical modulation of BRD4-PTEFb activity to control transcription.

RESULTS

Broad genome-wide changes in Pol II occupancy upon BRD4 depletion but not bromodomain inhibition

It has been demonstrated, both by RNA-seq and by measurement of nascent RNA associated with Pol II on chromatin (NET-seq), that the effect of the BET protein family inhibitor JQ1 differs from that of its PROTAC version, dBET6: while JQ1 bromodomain disruption has only a modest effect on Pol II pausing, dBET6-induced degradation of BRD2, BRD3, BRD4, and BRDT proteins leads to a dramatic, genome-wide increase in paused Pol II at promoters.²¹ To better understand the molecular mechanism underlying this disparity, we compared the effects of JQ1 or dBET6 treatment to that of acute and specific depletion of BRD4, the BET family member implicated in the regulation of Pol II pause release.^{12,29,30} To specifically deplete BRD4 without affecting other BET proteins, we generated an updated BRD4 degron line by modifying the published minilAA7 degron system (hereafter BRD4-IAA7) to reduce basal degradation seen with the standard auxin-inducible degron (AID)-tagged BRD4³¹ (Figures 1A and S1A). BRD4 was rapidly degraded upon auxin treatment in our updated line, and indeed basal degradation appears to be reduced compared to the BRD4-AID line (Figure S1B). Compared to auxin treatment in BRD4-IAA7, dBET6 treatment degrades BRD4 to a similar extent, while JQ1 treatment does not, as expected (Figure 1A). We then performed Pol II ChIP-seq upon auxin, JQ1, or dBET6 treatment in BRD4-IAA7 cells to assess the impacts of BRD4 degradation vs. bromodomain inhibition on the Pol II occupancy profile. As expected, dBET6 treatment phenocopied auxin treatment, inducing pausing at the majority of Pol II-transcribed genes, while JQ1 induced modest pausing (Figures 1B, 1C, and 1E). As shown by estimated cumulative density fraction (ECDF) and boxplot representations, as well as principal-component analysis (PCA) of the pause release ratios (PRR, reported as log₂ fold change), JQ1 treatment did not recapitulate the genome-wide Pol II pausing effect seen upon auxin or dBET6 treatment (Figures 1D and 1F–1H). As shown by scatterplot representation,

the gene-by-gene log₂PRR correlation with auxin treatment was much stronger for dBET6 than for JQ1, for which the change in PRR was poorly correlated with that of auxin treatment on a gene-by-gene basis (Figure S1C). An effect of JQ1 on pausing was pronounced at super enhancer-controlled genes such as MYC^{22,32} (Figure S1D). Since BRD4 is known to interact with PTEFb to phosphorylate Pol II,^{33,34} we also tested the effect of the potent CDK9 inhibitor NVP-2 in DLD-1 cells and found that CDK9 inhibition also induced strong Pol II pausing genome wide (Figure S1E). Taken together, these data demonstrated that bromodomain inhibition was not sufficient to abolish BRD4’s participation in Pol II pause release, suggesting that PTEFb might release Pol II through a BRD4-dependent but bromodomain-independent mechanism.

Bromodomains of BRD4 are dispensable for Pol II pause release in living cells

The finding that disruption of BRD4 binding to acetylated histone lysines was not sufficient to disrupt BRD4-mediated Pol II pause release (Figure 1) naturally led us to hypothesize that PTEFb could release Pol II in a BRD4-dependent but bromodomain-independent manner. To address this hypothesis, we generated stable lines with Dox-inducible, FLAG-tagged BRD4 constructs, including full-length (FL) BRD4 as well as bromodomain (ΔBD), ET (ΔET), or CTM (ΔCTM) domain deletion mutants, in BRD4-IAA7 cells. We also created a construct for a short, endogenously expressed BRD4 isoform (BRD4S) that also lacks the CTM (Figure 2A). GFP in the same backbone was used as a construct expression control. We first induced expression of the BRD4 constructs by Dox treatment for 2 days before rapidly depleting endogenous BRD4 with auxin for 3 h and then carried out Pol II ChIP-seq (Figure 2B). Surprisingly, we found that all three of the FL, ΔBD, and ΔET constructs could rescue the Pol II pausing caused by depletion of endogenous BRD4, while the ΔCTM and BRD4S constructs could not (Figure 2C). Genome-wide analysis of the Pol II ChIP-seq demonstrated a visibly inverted pattern of Pol II occupancy in cells expressing the ΔBD or ΔET but not ΔCTM constructs, indicating that although the ability of BRD4 to release Pol II is affected by CTM deletion, it is not affected by bromodomain or ET domain deletion (Figure 2D). As shown by boxplot and ECDF representations of log₂PRR, the ΔBD and ΔET mutant BRD4 constructs rescued Pol II release to an extent similar to that of WT (FL) BRD4, but ΔCTM and BRD4S did not (Figures 2E and 2F). Notably, upon addition of Dox, the signal from Pol II that is actively transcribing genome-integrated BRD4 constructs is observable in the Pol II ChIP-seq, confirming the expression of our mutant constructs (Figure S2A). We also tested Pol II serine 2 phosphorylation (Ser2P), a modification at the Pol II CTD that is strongly associated with the elongation stage,^{6,35} by ChIP-seq for the FL, ΔBD, and ΔCTM rescue conditions. Consistent with the total Pol II ChIP-seq, FL and ΔBD constructs could rescue the loss of Ser2P signal caused by depletion of endogenous BRD4, while ΔCTM could not (Figures 2G and 2H). We did observe several genes (such as MYC) that were not fully rescued by the bromodomain-less BRD4, reflecting the pausing effect of JQ1 treatment at some genes (Figure S2B). We performed genome-wide K-means clustering to identify the “MYC-like” genes, but did not observe

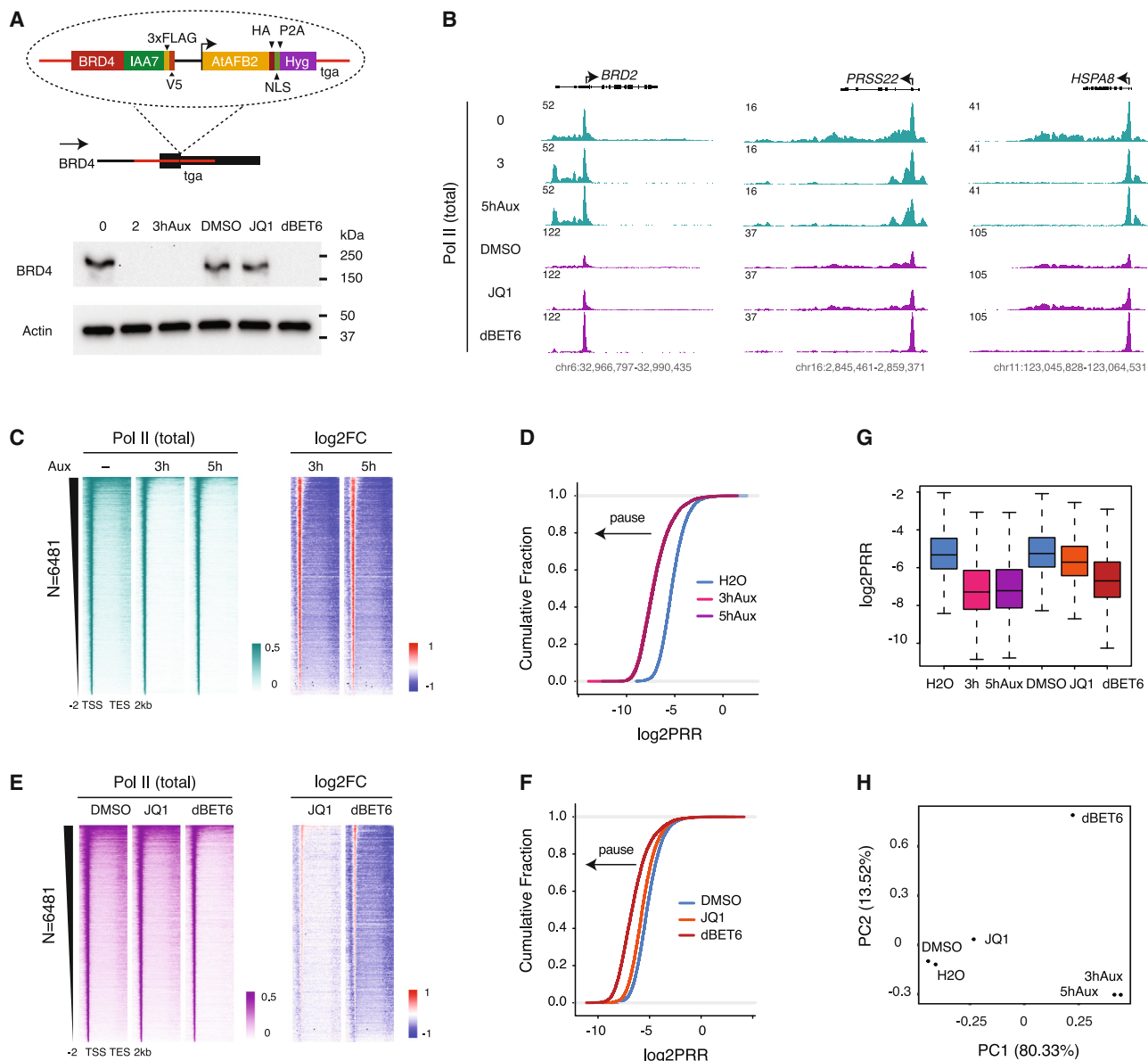


Figure 1. Broad Pol II pausing upon BRD4 depletion but not bromodomain inhibition

(A) Schematic of the updated BRD4-IAA7 degron line. The F box protein AtAFB2 was integrated into the C terminus of the BRD4 locus under the control of an independent promoter. Western blot indicating the acute depletion of BRD4 by auxin (500 µM) or dBET6 (250 nM) treatment but not JQ1 (1 µM) in the BRD4-IAA7 degron line is shown. Cells were treated with auxin for 2 or 3 h, or with JQ1 or dBET6 for 3 h. These treatment concentrations/durations are relevant to all of Figure 1.

(B) Genome browser track examples of total Pol II ChIP-seq signal at the representative genes *BRD2*, *PRSS22*, and *HSPA8* upon auxin treatment (0, 3, or 5 h) or upon JQ1 or dBET6 treatment (3 h).

(C) Heatmap showing the genome-wide Pol II occupancy profile upon auxin treatment and the profile of fold change in Pol II occupancy compared to control, in which the differential between promoter (increased occupancy, red) and gene body (reduced occupancy, blue) indicates paused Pol II. The gene list ($N = 6,481$) in this analysis is used throughout the study (except for Figures 3H–3J).

(D) Estimated cumulative density function (ECDF) of pause release ratios (PRR, reported as \log_2 fold change) for auxin treatment vs. untreated control. The PRR is the ratio of Pol II occupancy within gene bodies to its occupancy at promoters. A leftward shift of the curve indicates an increase in the frequency and/or duration of promoter-proximal pausing, while a rightward shift indicates reduced pausing and/or more efficient release into gene bodies.

(E) Heatmap showing the genome-wide Pol II occupancy profile upon JQ1 or dBET6 treatment and the profile of fold change in occupancy vs. control.

(F) ECDF of the \log_2 PRR upon JQ1 or dBET6 treatment.

(G) Boxplot of the \log_2 PRR for auxin, JQ1, and dBET6 treatment.

(H) PCA analysis of the \log_2 PRR for auxin, JQ1, and dBET6 treatment.

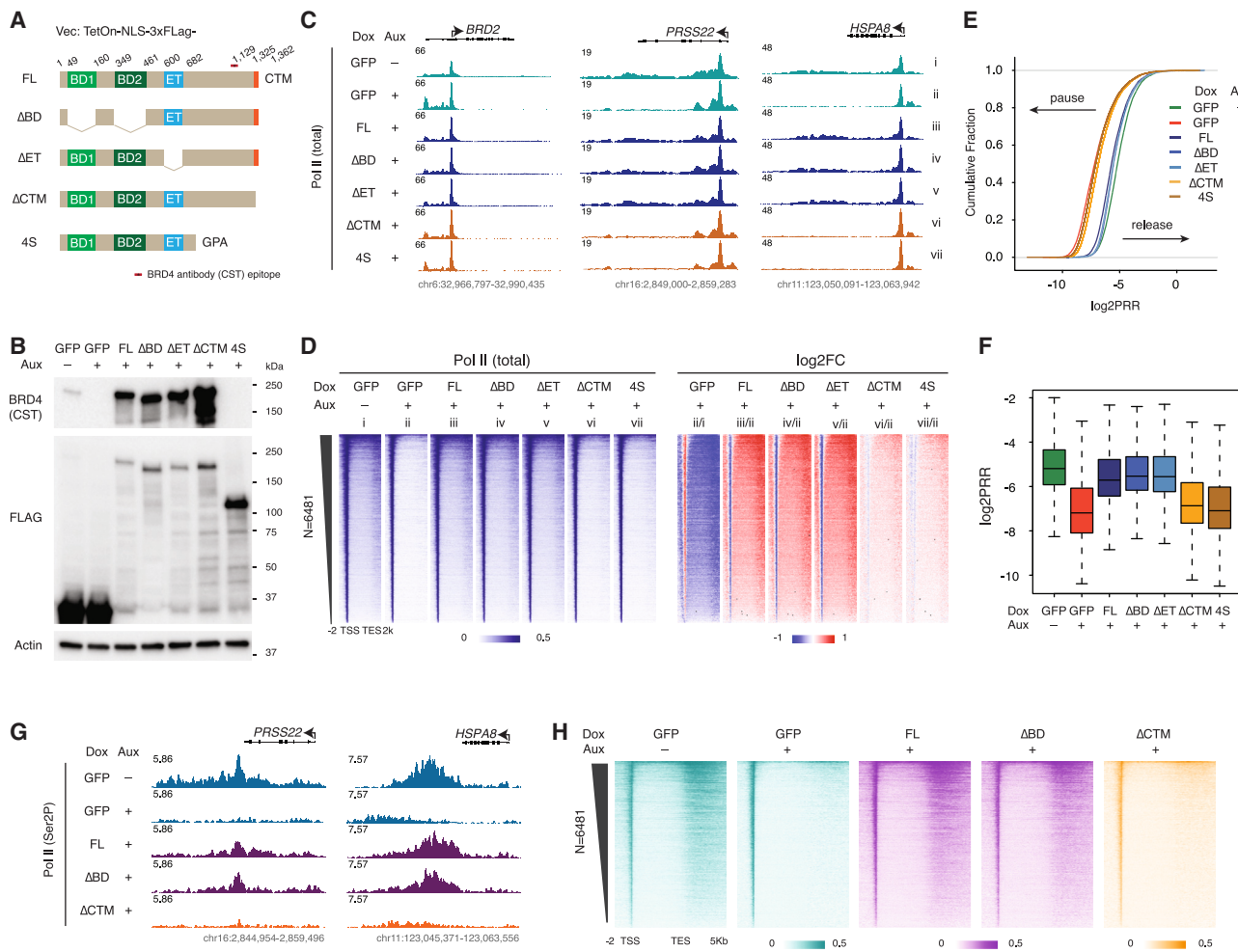


Figure 2. BRD4 bromodomains are dispensable for Pol II pause release

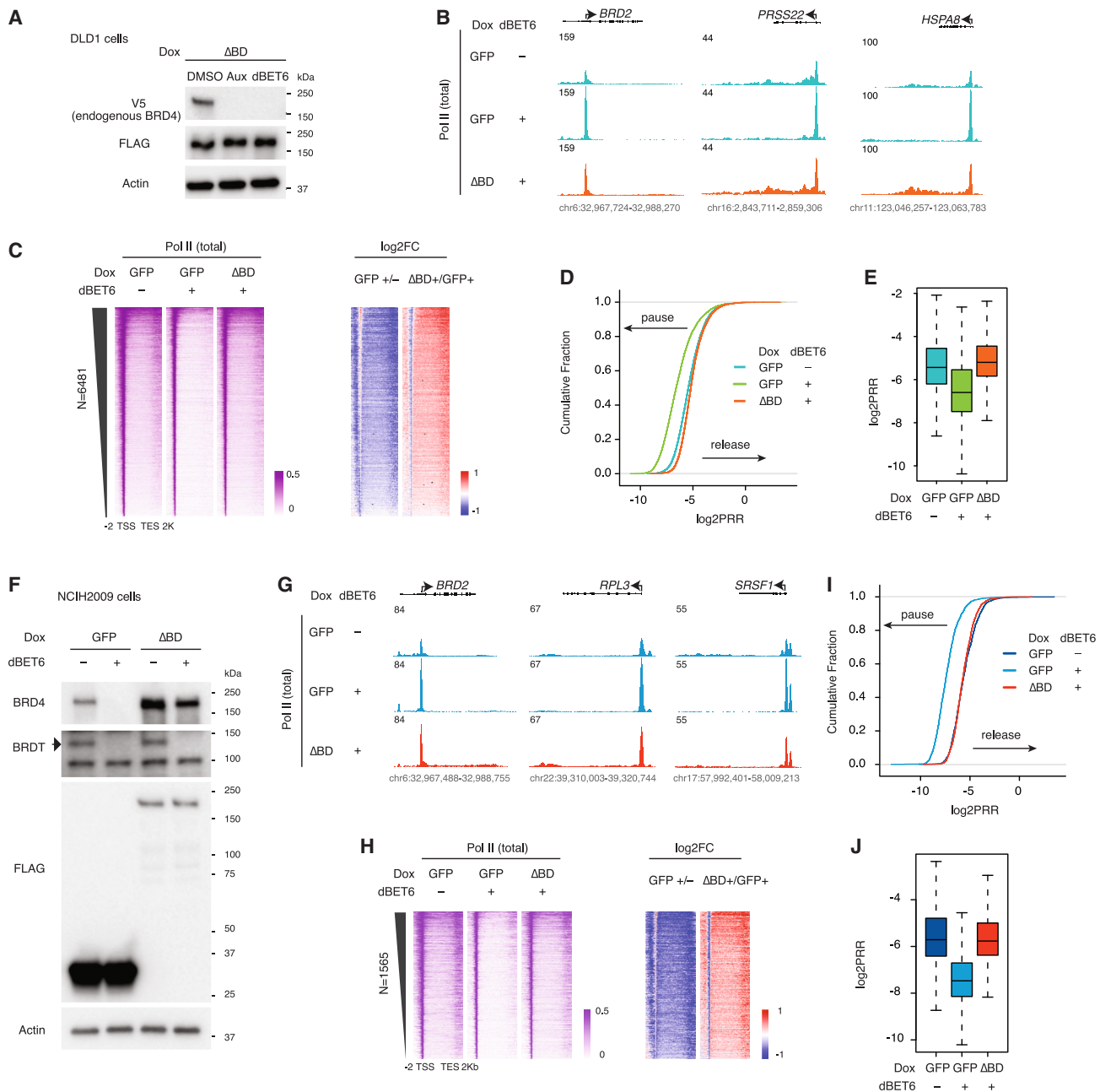
- (A) Schematic of the FLAG-tagged, Dox-inducible BRD4 mutant constructs, relevant to all of Figure 2 (vector: TetOn-NLS-3xFLAG). The location of the epitope for the commercial BRD4 antibody (CST #13440) is indicated.
- (B) Western blot showing BRD4 mutant construct expression in the same conditions used for subsequent rescue experiments: auxin-treated (3 h) BRD4-IAA7 cells, 2 days after Dox treatment (50 nM). Blot was probed for BRD4 using antibodies against a C-terminal epitope (see A) and the N-terminal FLAG tags.
- (C) Track examples showing the total Pol II ChIP-seq signal at the *BRD2*, *PRSS22*, and *HSPA8* loci for the rescue experiment, in which auxin-induced endogenous BRD4 depletion is complemented by Dox-induced mutant construct expression.
- (D) Heatmaps showing the genome-wide Pol II occupancy and fold change in occupancy for mutant constructs vs. GFP control in the rescue experiment.
- (E) ECDF comparison of log₂PRR in the rescue experiment showing ΔCTM and BRD4S mutant constructs clustered with auxin-treated (BRD4-depleted) GFP control, while FL, ΔBD, and ΔET constructs are clustered with the untreated GFP control.
- (F) Boxplot comparison of log₂PRR in the rescue experiment.
- (G) Track examples of the Pol II Ser2P ChIP-seq signal at the *PRSS22* and *HSPA8* loci, showing loss of Pol II Ser2P occupancy due to auxin-induced endogenous BRD4 depletion that is rescued by Dox-induced expression of the FL or ΔBD but not ΔCTM mutant constructs.
- (H) Heatmaps showing the genome-wide Ser2P occupancy under the same rescue experiment conditions.

notable differences between rescue by FL and ΔBD constructs. When calculating the log₂FC of the PRR and Pol II occupancy at the gene body, we found that only four genes met a stringent cutoff (log₂FC of PRR FL vs. ΔBD ≥ 1 and log₂FC of Pol II occupancy FL vs. ΔBD ≥ 1). These four genes are *MYC*, *KRT80*, *CXCL5*, and *SYT8*. However, 49 genes met a less stringent cutoff (≥ 0.585) (Table S1). Next, we tested the ability of the mutant constructs to rescue cell growth and confirmed that the bromodomain-less constructs can rescue the cell growth defect caused by endogenous BRD4 depletion (Figure S2C). We also carried

out RNA-seq for the rescue experiment after 24 h of BRD4 depletion and found 863 down-regulated genes that were rescued by bromodomain-less mutants but not the ΔCTM mutant, further supporting the transcriptional relevance of our conclusion at the level of Pol II occupancy and pause release (Figure S2D).

Bromodomain dispensability is conserved across cell lines

Since the bromodomain-less mutant BRD4 is resistant to dBET6 treatment (Figure 3A), we treated cells expressing the

**Figure 3. Bromodomain dispensability conserved across cell lines**

- (A) Western blot showing degradation of endogenous BRD4 (V5) but not the bromodomain-less BRD4 mutant (FLAG) upon auxin or dBET6 treatment in the BRD4-IAA7 DLD-1 degron line.
- (B) Track examples of the total Pol II ChIP-seq signal at the *BRD2*, *PRSS22*, and *HSPA8* loci after dBET6 treatment and rescue by bromodomain-less BRD4 in DLD-1 cells.
- (C) Heatmap showing the genome-wide Pol II occupancy and fold change in occupancy for the bromodomain-less mutant construct vs. GFP control after dBET6 treatment in DLD-1.
- (D) ECDF of the log₂PRR from the total Pol II ChIP-seq for the dBET6 rescue experiment in DLD-1.
- (E) Boxplot of the log₂PRR from the total Pol II ChIP-seq for the dBET6 rescue experiment in DLD-1.
- (F) Western blot showing the depletion of endogenous BRD4 and BRDT, but not the bromodomain-less mutant, by dBET6 treatment (3 h) in NCI-H2009 cells.
- (G) Track examples of the total Pol II ChIP-seq signal upon dBET6 treatment (3 h) and rescue by bromodomain-less BRD4 in NCI-H2009 cells.
- (H) Heatmap showing the Pol II occupancy profiles and corresponding fold changes across the 1,565 genes for which dBET6 causes strong pausing (2-fold reduction of Pol II at gene bodies and 2-fold reduction of PRR), rescued by bromodomain-less BRD4 in NCI-H2009.
- (I) ECDF of the log₂PRR from the Pol II ChIP-seq for the dBET6 rescue experiment in NCI-H2009 (N = 1,565).
- (J) Boxplot of the log₂PRR from the Pol II ChIP-seq for the dBET6 rescue experiment in NCI-H2009 (N = 1,565).

(legend continued on next page)

bromodomain-less mutant with dBET6 to see whether the mutant could reverse the pausing effect normally seen upon dBET6 treatment. As expected, we found that dBET6-induced pausing is abolished by bromodomain-less BRD4 (Figures 3B–3E). We then tested whether this effect holds true beyond DLD-1 cells by expressing the bromodomain-less mutant and testing the effect of dBET6 in a very different cell line, NCI-H2009. In addition to BRD4, the NCI-H2009 cells also endogenously express the BET family member BRDT, but both proteins are degraded by dBET6 (Figures 3F, S3A, and S3B). The genome-wide Pol II profile differs between DLD-1 and NCI-H2009, but we found that for most genes displaying dBET6-induced pausing in NCI-H2009, this effect can be rescued by reconstitution with the bromodomain-less mutant (Figure 3G). Genome-wide analysis in NCI-H2009 further supported our conclusion that the bromodomain-less mutant rescues Pol II pause release in NCI-H2009 cells (Figure S3C). Out of 6,481 genes, a total of 1,565 dBET6-paused genes (24.15%) were selected using a dual threshold: 2-fold reduction of Pol II at gene bodies and 2-fold reduction of PRR. We repeated the same analysis with these genes and found that most of the highly paused genes were rescued by the bromodomain-less BRD4 in NCI-H2009 cells (Figures 3H–3J). Although the role of BRDT in transcription is largely unknown, it contains a PTEFb-interacting domain and could potentially function similarly to BRD4 in releasing paused Pol II, and bromodomain-less BRD4 may also rescue the effect of BRDT depletion in NCI-H2009 cells. Nevertheless, our data indicate that the bromodomain-independent function of BRD4 in Pol II release is not strictly limited to DLD-1 cells.

A bromodomain-less BRD4 C-terminal fragment interacts with PTEFb and rescues Pol II pause release

To investigate which BRD4 regions are required for the function of BRD4 in Pol II pause release, we generated a series of N-terminal truncation mutants retaining the CTM in the same FLAG-tagged vector as above (Figure S3D). After validating the induced expression of these mutants (Figure S3D), we used Pol II ChIP-seq to screen them using the same rescue experiment setup, with the bromodomain deletion mutant (Δ BD) as a negative control. To our surprise, the Pol II profile was similar for all the mutant constructs, with a noticeable decrease in gene body Pol II occupancy for only the shortest mutant construct (Cs), which consists of just 170 residues from the C terminus of BRD4 (Figures S3E and S3F). We calculated the \log_2 PRR and found that all the truncation mutants could rescue Pol II release to an extent equal or greater to that of the Δ BD construct, as indicated in the boxplot representation (Figure S3G). The endogenous BRD4 acquired a 3xFLAG tag upon IAA7 tagging, so to exclude any potential confusion deriving from residual endogenous BRD4, we replaced the 3xFLAG tag with GFP for further characterization of the C-terminal constructs (Figure 4A) (in our previous experience, FLAG ChIP-seq works poorly in DLD-1 cells, while GFP ChIP-seq works well). We first validated the expression of the GFP-tagged shortest construct (Cs), Cs with CTM deletion (Cs Δ CTM), and a CTM-only (CTM) construct by western blot (Figure S4A). Then, we carried out immunoprecipitation followed by mass spectrometry (IP-MS) for these mutants. The consistent results of two replicate IP-MS experiments showed that only the Cs mutant retained the

ability to interact with PTEFb (Figure 4B). We assessed the Cs interactome, represented by interacting protein q value vs. their enrichment over that of the vector, and found that two of the most outstanding Cs-interacting proteins are components of the PTEFb complex, which we then validated by western blot analysis (Figures 4C and 4D). We further validated these results by carrying out Pol II ChIP-seq for the GFP-tagged mutant constructs in comparison with FL BRD4. Consistently, the Pol II occupancy profile shows the rescue of Pol II pause release by the Cs construct (Figures 4E and 4F). Consistent with the FLAG-tagged version, despite noticeable reduction in gene body Pol II occupancy for the Cs mutant, there was no corresponding defect in the Cs PRR relative to the FL BRD4 positive control (Figures S4B–S4D). Since the PRR was actually highest for the extended C terminus (C) in our screen of FLAG-tagged mutant constructs (Figure S3G), we also generated a GFP-tagged C construct (Figure 4A) and compared its ability to rescue Pol II release to the FL and Δ BD constructs, finding no obvious defect in rescued Pol II occupancy at the gene body relative to the BRD4-FL positive control (Figures S4E–S4I). We also confirmed the functionality of the C terminus by Ser2P ChIP-seq in the rescue experiment (Figures 4G and 4H). Multiple replicates of IP-MS, Pol II ChIP-seq, and Ser2P ChIP-seq experiments reproducibly consolidated our conclusion that the C terminus of BRD4 is sufficient for the release of paused Pol II.

Distinct layers of the BRD4-PTEFb complex: Identification of a histone acetylation-independent but active BRD4-PTEFb population

The extent to which BRD4 is required for recruiting PTEFb to chromatin and regulating gene expression remains a subject of some debate.^{21,34,36} Aiming to further investigate this point, we carried out ChIP-seq for Pol II, CCNT1, and CDK9 in BRD4-IAA7 cells with and without prior depletion of endogenous BRD4 by auxin treatment. BRD4 depletion led to a dramatic reduction in the CCNT1 peaks at promoters genome-wide, indicating that CCNT1 recruitment to chromatin relies on BRD4 (Figures 5A and S5A) but not vice versa, as CDK9 depletion leads to increased BRD4 ChIP signal (Figures S5C and S5D). We integrated these data with our previously published ChIP-seq in the BRD4-AID line and compared the peaks of CCNT1 and BRD4 to H3K27ac (Figure 5A). Genome-wide analysis revealed general colocalization of CCNT1 and BRD4 at promoters, which was mostly associated with histone acetylation (Figures 5B and 5C). Signal was generally low in our CDK9 ChIP-seq, but at genes that were highly enriched with Pol II we were able to see CDK9 peaks with the same trend seen for CCNT1 (Figures S5A and S5B). Notably, a few genes show increased Pol II occupancy and thus retain PTEFb upon BRD4 depletion (Figure S5A), which is presumably recruited by SEC (data not shown). Next, we carried out GFP ChIP-seq for the GFP-tagged BRD4-FL and mutants (Figure 4A). Surprisingly, although they could all rescue Pol II occupancy and release, the Δ BD, C, and Cs mutants had ChIP-seq signals that were minimal genome-wide compared to that of the FL BRD4 (Figures 5D and S5E). We tried several different ChIP-seq conditions with increasing amounts of chromatin but were not able to obtain clear peaks for all bromodomain-less BRD4 mutants. We then checked CCNT1 occupancy

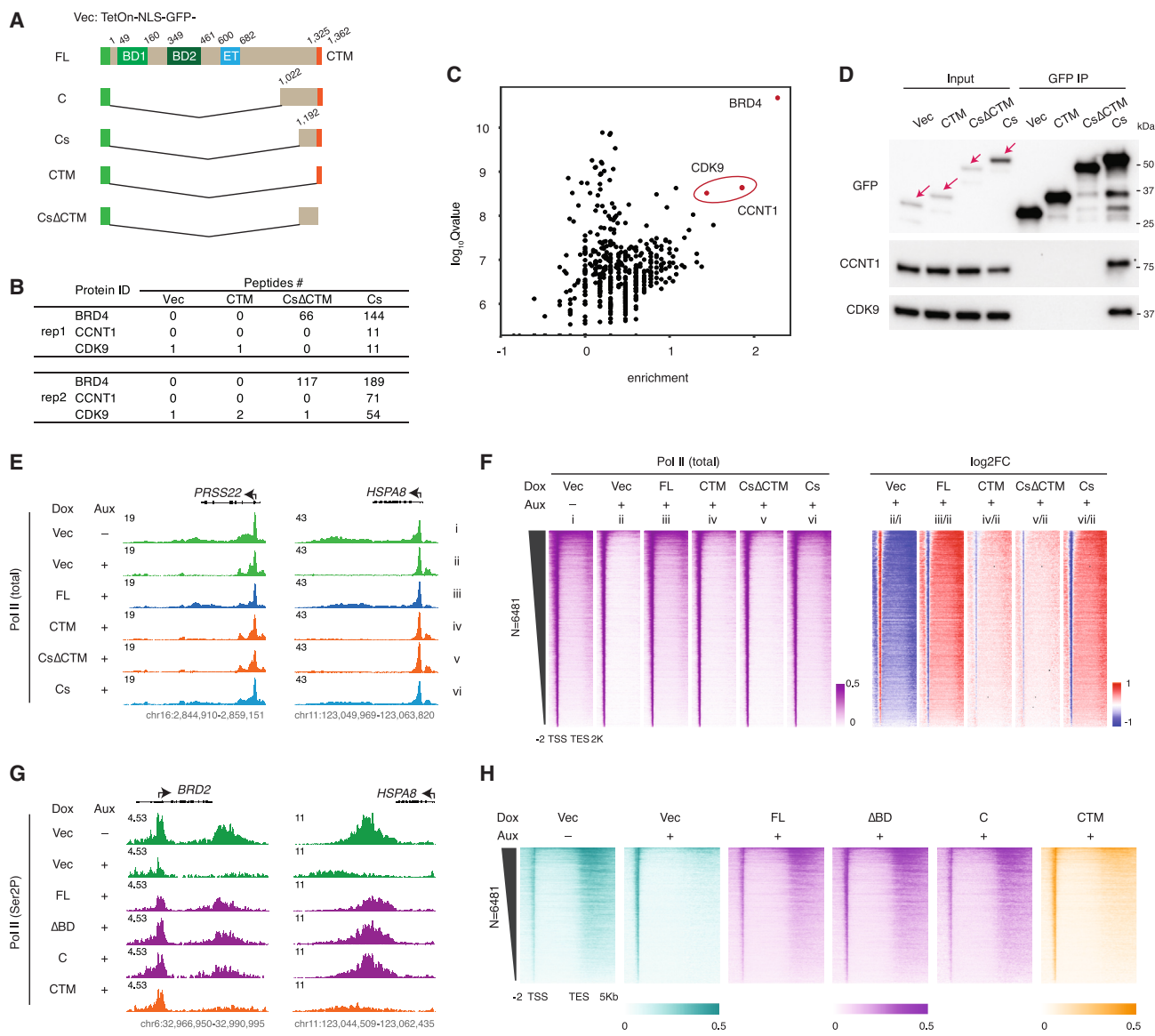


Figure 4. BRD4 C-terminal fragment interacts with PTEFb and rescues Pol II pause release

- (A) Schematic of the GFP-tagged FL BRD4 and BRD4 C terminus constructs (vector: TetOn-NLS-GFP). Cs, short C terminus.
- (B) GFP IP-MS results showing peptide counts for the bait (BRD4) and PTEFb complex components (CCNT1 and CDK9) in two replicates after Dox (50 nM)-induced expression of vector, CTM, CsΔCTM, or Cs mutant constructs for 2 days. Note that the 0 bait peptide count for the CTM construct is probably due to impaired peptide alignment, as the CTM construct is itself a (GFP-tagged) peptide of only 37 residues.
- (C) Scatterplot showing the \log_{10} q value vs. the enrichment over vector (calculated by $\log_{10}\text{FC}$ of peptide counts +1) for the BRD4-Cs-interacting proteins in the second GFP IP-MS replicate.
- (D) Western blot validating the GFP IP-MS result using the elute from the second replicate.
- (E) Track examples for total Pol II ChIP-seq signal at the *PRSS22* and *HSPA8* gene loci upon auxin treatment and rescue by different GFP-tagged mutants.
- (F) Heatmap showing the genome-wide Pol II occupancy profile and the corresponding fold changes for the GFP-tagged rescue experiment.
- (G) Track examples for Ser2P ChIP-seq signal at the *BRD2* and *HSPA8* gene loci upon auxin treatment and rescue by different GFP-tagged mutants.
- (H) Heatmap showing the genome-wide Ser2P occupancy profile for the GFP-tagged rescue experiment.

in the rescue experiments and found that CCNT1 signal was restored by BRD4-FL but not the bromodomain-less C mutant (Figure 5E). This result is consistent with the GFP ChIP-seq results and further indicates that the population or “layer” of acetylation-bound BRD4-PTEFb captured by ChIP-seq is mainly

associated with BRD4 bromodomains interacting with acetylation sites, while a distinct acetylation-independent layer, which could be too dynamic to be efficiently captured by ChIP-seq, nevertheless functions to release Pol II (Figures 4E and 4G). To further confirm that disruption of the acetylation-bound

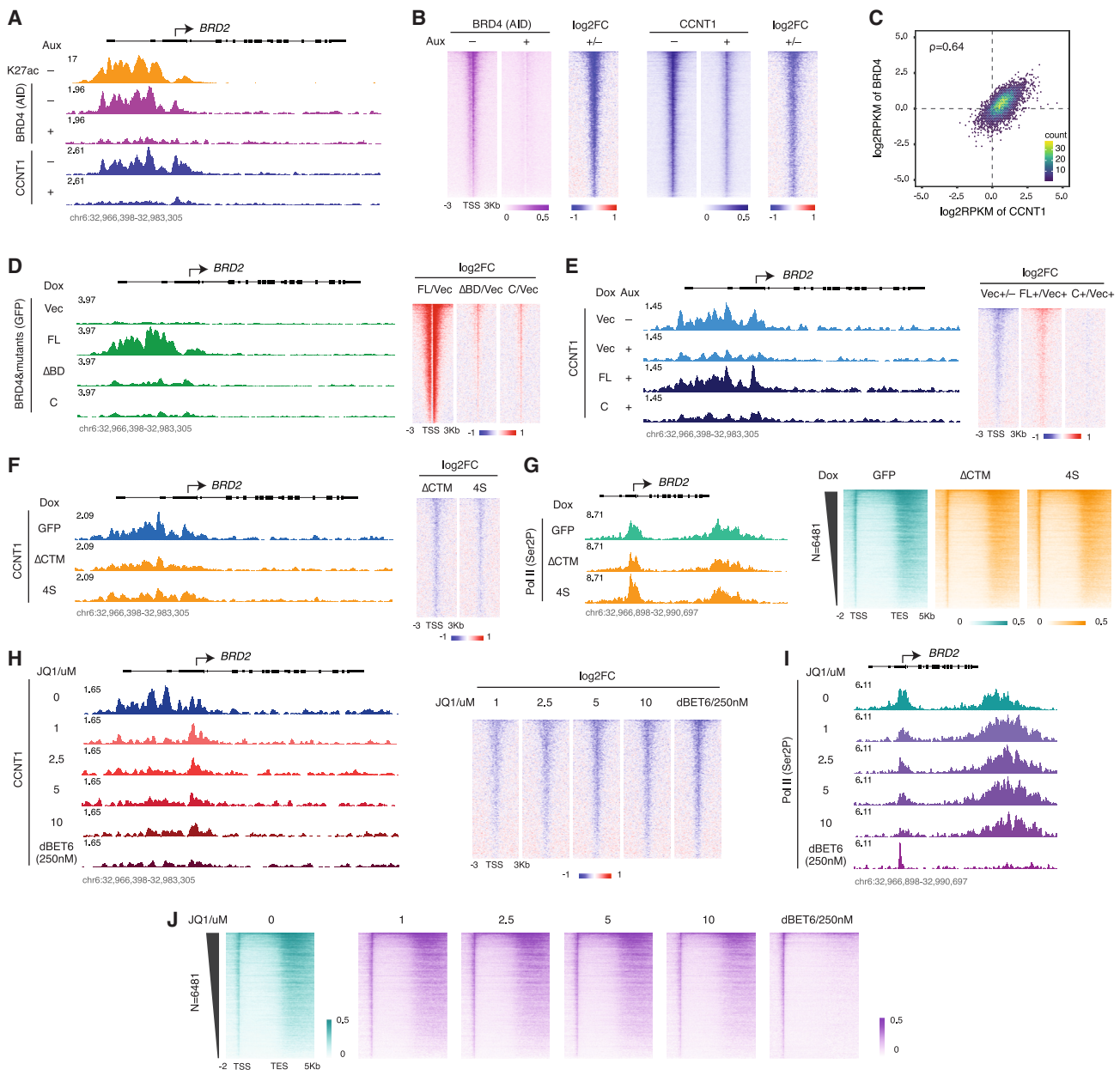


Figure 5. Identification of a distinct BRD4-PTEFb population: Active but not histone acetylation bound

- (A) Track examples for AID ChIP-seq in the BRD4-AID line and CCNT1 ChIP-seq in the BRD4-IAA7 line with/without auxin treatment (3 h). H3K27ac ChIP-seq signal in the BRD4-AID line is shown for comparison.
- (B) Heatmap showing the genome-wide BRD4 and CCNT1 occupancy profile and the corresponding fold change upon auxin treatment for the conditions in (A). Genes are ranked by BRD4 signal in the untreated control.
- (C) Scatterplot showing the relative promoter density of CCNT1 vs. BRD4, calculated by the \log_2 RPKM of the ChIP-seq signals at the regions flanking (± 1 kb) the Pol II pausing sites.
- (D) Track examples for GFP ChIP-seq signal upon induction of GFP-tagged BRD4-FL or the indicated mutants (left). Heatmap showing the genome-wide fold changes of the GFP-tagged BRD4 mutants relative to the vector is shown at right. The endogenous BRD4 was depleted by auxin treatment (3 h) in all samples. Genes are ranked by GFP signal in the GFP-BRD4-FL condition.
- (E) Track examples for CCNT1 ChIP-seq signal upon endogenous BRD4 depletion and rescue with indicated GFP-tagged mutants (left). Heatmap showing the genome-wide CCNT1 fold changes is shown at right. Genes are ranked by CCNT1 signal in the untreated vector control.
- (F) Track examples for the CCNT1 ChIP-seq signal upon induction of the FLAG-tagged, CTM-less BRD4 mutants by Dox treatment for 2 days (left). Heatmap showing the genome-wide profile of fold changes in CCNT1 occupancy is shown at right. Genes are ranked by CCNT1 signal in the GFP control.
- (G) Track examples for the Ser2P ChIP-seq from the same samples as in (F) (left). Heatmap showing the corresponding genome-wide Ser2P occupancy profile is shown at right.

(legend continued on next page)

BRD4-PTEFb layer alone could not abolish Pol II pause release, we exogenously overexpressed the CTM-less (and therefore PTEFb-blind) BRD4 mutants to displace the population of acetylation-bound BRD4-PTEFb. Indeed, a significant amount of BRD4-PTEFb was knocked off from chromatin by overexpression of either the ΔCTM or 4S CTM-less BRD4 mutants (Figure 5F). However, this displacement did not constitute a dominant-negative effect, as the ChIP-seq signals for both total Pol II and Ser2P were not noticeably diminished by CTM-less construct overexpression (Figures S5F–S5H and 5G). To further validate this observation with a more severe disruption of the acetylation-bound layer, we then treated cells with increasing concentrations of JQ1. We also included dBET6 treatment as a control for joint disruption of both the acetylation-bound and acetylation-independent layers. Though CCNT1 ChIP-seq signals decreased dramatically with increasing concentrations of JQ1, concomitant change in the Ser2P ChIP-seq signals was minimal, and only with dBET6 disruption of both layers did Ser2P signal fade away (Figures 5H–5J). These results suggest that disruption of the acetylation-independent BRD4-PTEFb layer is the underlying mechanism by which dBET6 differs from JQ1 in effectively abolishing Pol II pause release.

The BRD4 C-terminal disordered region is required for cyclin T1 binding in the BRD4-PTEFb complex

The fact that the GFP-tagged CTM cannot pull down PTEFb, while the extended Cs can, prompted us to investigate how the C terminus of BRD4 mediates its interaction with PTEFb. We first carried out GFP IP for the GFP-tagged, FL BRD4 upon dCDK9 treatment. CDK9 degradation also impairs BRD4-CCNT1 interaction, indicating the requirement of CDK9 for stable BRD4-PTEFb complex formation (Figure 6A). We then generated GFP-tagged partial (ΔCdp) and entire (ΔCd) C terminus deletion mutants (Figures 6B and S6A). Ser2P ChIP-seq in the rescue experiment revealed that though Pol II-releasing activity was largely impaired in the partial deletion mutant, the entire deletion almost completely abolished activity (Figures S6B and S6C). We carried out GFP IP for the ΔCd mutant and found a severe loss of binding to CCNT1 but not CDK9 compared to the FL and C mutants (Figure 6C), which could explain why the ΔCd mutant cannot rescue Pol II release, as was further confirmed by the total Pol II ChIP-seq (Figures 6D–6G). Finally, we computed the predicted structure of the CTM of BRD4 (37 residues) in association with the PTEFb complex (the initial 344 N-terminal residues of CDK9 and the initial 293 N-terminal residues of CCNT1, as the corresponding crystal structure has been published³⁷) using AlphaFold integrated in ChimeraX.³⁸ In line with the results of this study, the predicted structure highlights a critical role for the CTM in mediating the interaction between BRD4 and PTEFb, with CTM protruding into the pocket created by CDK9 and CCNT1 (Figure 6H).

DISCUSSION

In this study, we sought to determine why broad genome-wide changes in Pol II occupancy are seen upon BRD4 depletion but not bromodomain inhibition. Our depletion and rescue strategy allowed us to directly compare exogenous WT BRD4 with mutant BRD4 constructs, including bromodomain-less mutant BRD4 constructs that are unable to bind acetylated histone lysine residues. By characterizing the effects of these constructs on the chromatin-associated profiles of Pol II and its elongating Ser2P form, we determined that while the C terminus of BRD4 is required for its participation in Pol II pause release, BRD4 bromodomains are dispensable for this function. We further validated the essential role for the BRD4 C terminus, isolating a minimal C-terminal fragment that lacks bromodomains but physically interacts with PTEFb, and showing that cellular expression of this C-terminal fragment is sufficient to replicate the role of FL BRD4 in Pol II pause release. Displacing endogenous BRD4 from chromatin by overexpressing PTEFb-blind mutants reduced PTEFb chromatin occupancy without affecting Pol II pause release, phenocopying the effect of bromodomain inhibitor treatment. Importantly, this result indicates that endogenous bromodomain-containing BRD4 can release paused Pol II irrespective of its association with acetylated histones. The endogenous expression of the BRD4 short isoform (4S), which lacks the CTM required for PTEFb interaction and thus cannot participate in release of paused Pol II, suggests that this displacement is physiologically relevant.

Our results all support a previously unappreciated role for BRD4 in acetyl recognition-independent release of paused Pol II. In the model emerging from our results (Figure 7), there are two distinct populations or “layers” of BRD4-PTEFb: a first layer of acetylation-bound BRD4-PTEFb, complemented by a second layer of acetylation-independent BRD4-PTEFb that effectively releases paused Pol II. One question emerging from this model is what role the prominent acetylation-bound BRD4-PTEFb layer plays in transcription. Further studies are needed to dissect the endogenous functions of FL BRD4 and its short isoform, which could potentially balance the two layers of BRD4-PTEFb. Nevertheless, this angle on BRD4 function brings clarity to the long-running debate concerning the causes of insensitivity or resistance to BET inhibitors, which has previously been observed in multiple studies and trials.^{39–41} Notably, other studies have also shown that BRD4 is required for survival even in BET inhibitor-resistant cells, similarly implicating a function for BRD4 beyond that mediated by its bromodomains.^{39,42,43} Our findings represent a major step toward mechanistic understanding of this function, as they reveal the crucial importance of BRD4’s C terminus for CDK9/CCNT1 interaction and regulation of Pol II pause release. Future studies will be focused on determining the structural basis of the interaction of BRD4 with CDK9 and CCNT1 and developing BRD4 C-terminus specific inhibitors, which (unlike

(H) Track examples for the CCNT1 ChIP-seq in a series concentration of JQ1 and 250 nM dBET6 treatment for 3 h in the BRD4-IAA7 cells (left). Heatmap showing the corresponding genome-wide CCNT1 fold changes relative to DMSO treatment is shown at right. Genes are ranked by CCNT1 signal in the DMSO control.

(I) Track examples for the Ser2P ChIP-seq from the same JQ1 or dBET6-treated samples as in (H).

(J) Heatmap showing the corresponding genome-wide Ser2P occupancy profile.

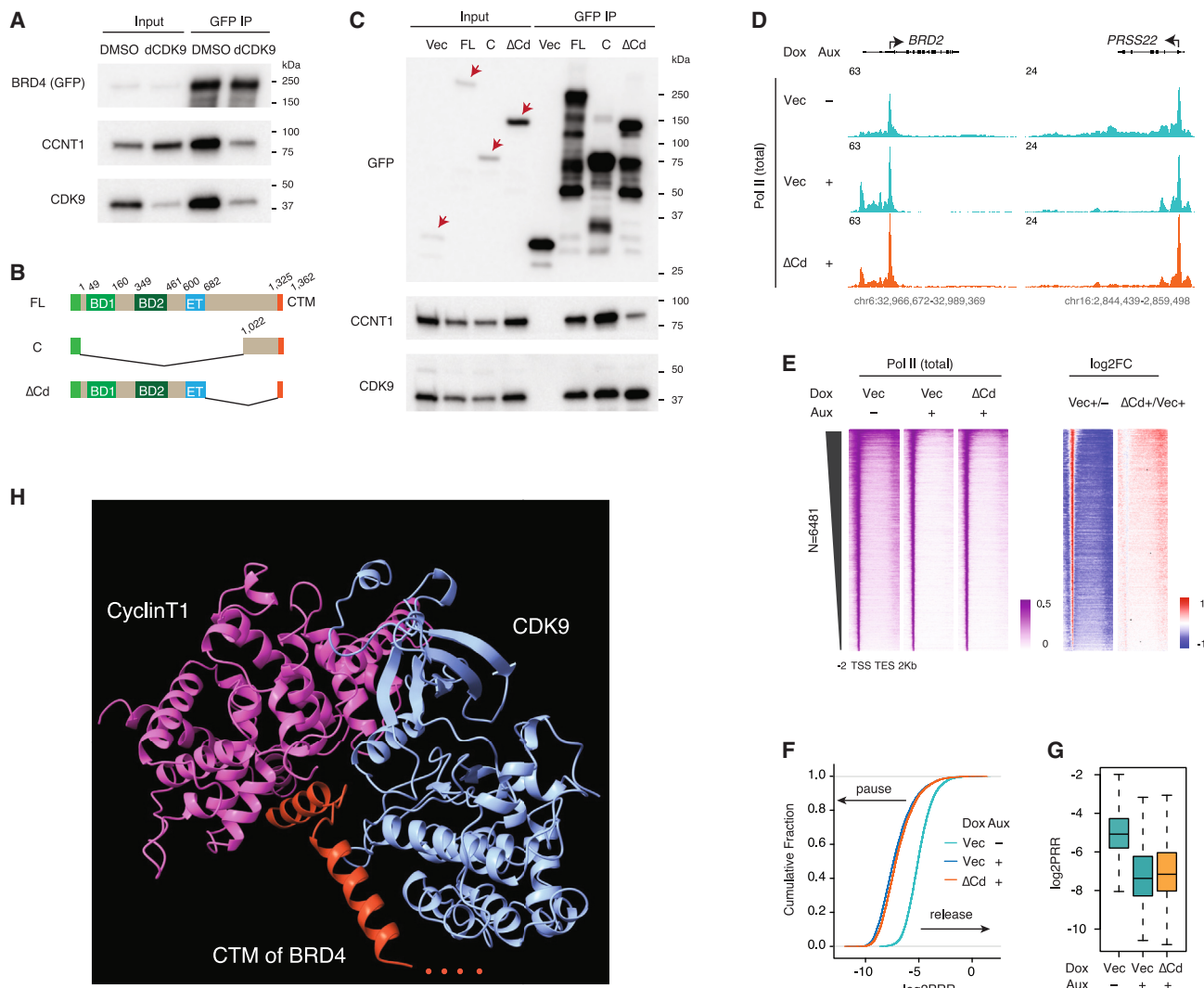


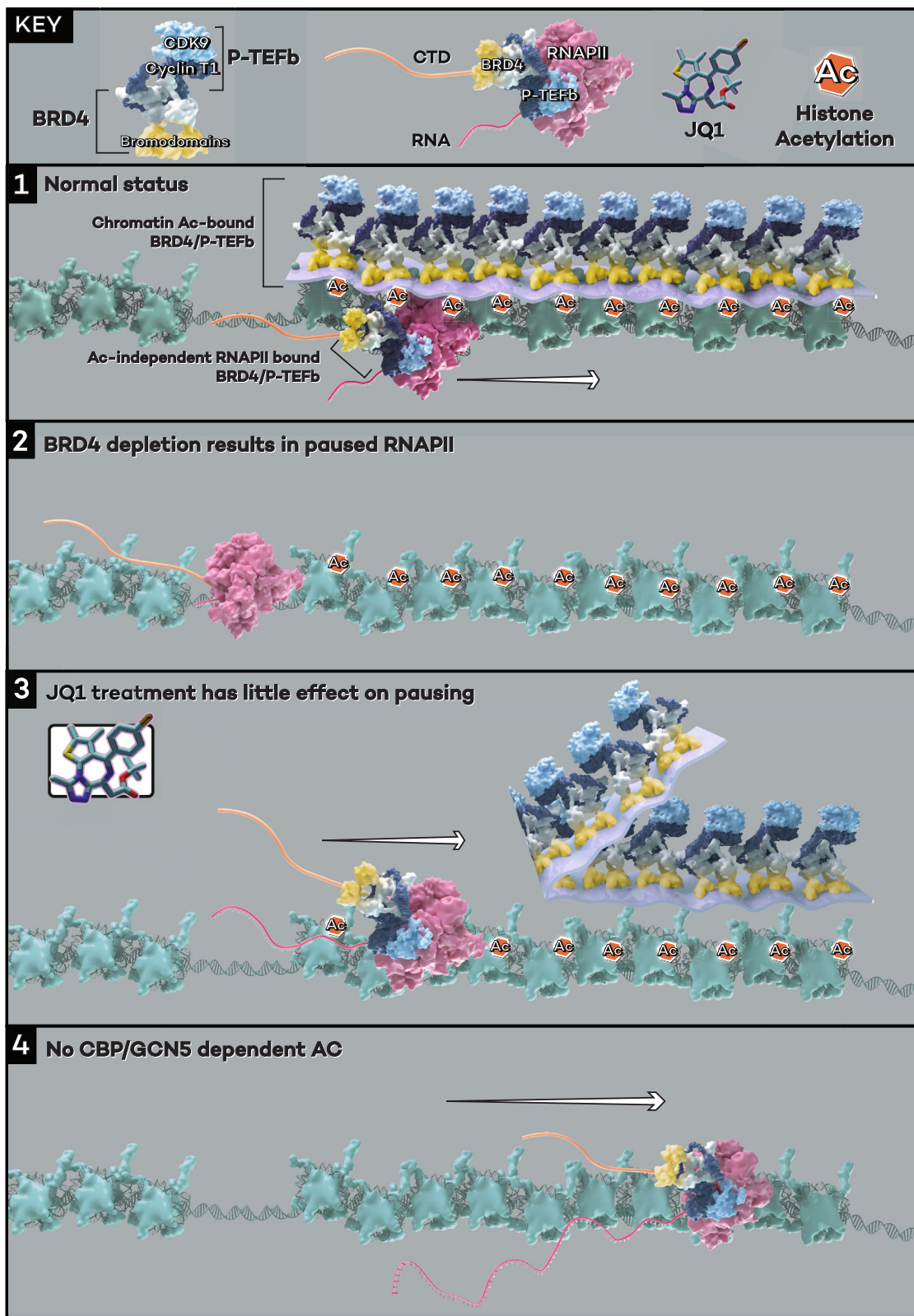
Figure 6. The BRD4 C terminus stabilizes cyclin T1 in the BRD4-PTEFb complex

- (A) Western blot of GFP IP showing the PTEFb complex components associated with BRD4 upon dCDK9 (2.5 μM) treatment for 3 h. GFP-tagged BRD4-FL was induced by Dox treatment for 2 days.
- (B) Schematic of the GFP-tagged constructs: BRD4-FL, BRD4-C, and BRD4-ΔCd (deletion of the C-terminal disordered region).
- (C) Western blot of GFP IP showing PTEFb complex components associated with BRD4 and its C terminal mutants. GFP-tagged BRD4-FL and mutant constructs were induced by Dox treatment for 2 days. Endogenous BRD4 was depleted in all samples by auxin treatment (3 h) prior to IP.
- (D) Track examples for the total Pol II ChIP-seq signal upon BRD4 depletion and rescue by BRD4-ΔCd.
- (E) Heatmap showing the genome-wide Pol II occupancy and the corresponding fold changes for the rescue experiment in (D).
- (F) ECDF showing the log₂PRR for the Pol II ChIP-seq for the rescue experiment in (D).
- (G) Boxplot showing the log₂PRR for the Pol II ChIP-seq for the rescue experiment in (D).
- (H) AlphaFold-predicted structure for CTM of BRD4 and the PTEFb complex (344 CDK9 N-terminal residues, 293 CCNT1 N-terminal residues, and 37 C-terminal BRD4 residues were used for the computational prediction).

pan-BET inhibitors⁴⁴) would leave the acetylation-bound layer of BRD4 and other BET family proteins unaffected. We predict that this class of inhibitors will be highly efficient in abolishing the function of BRD4 in Pol II pause release, resulting in potent therapeutic benefit.

In line with the bromodomain-independent function of BRD4, Sankar et al. mutated all 28 H3 alleles from K27 to R27 to show that H3K27 modification is not required either for proper

loading of the Pol II machinery onto chromatin or for transcriptional activation during cell fate transition in murine embryonic stem cells.²⁶ Similarly, Zhang et al. found that abolishing H3K27ac was not sufficient to disrupt enhancer activity.²⁷ Narita et al. used nascent RNA-seq to characterize the immediate transcriptional outcome of inhibiting p300/CBP enzymatic activity via the small molecule A-485. For the majority of nascent transcripts, abundance remained unaltered by enzymatic inhibition



(legend on next page)

even at high A-485 doses that induce an observable decrease in H3K27ac genome wide.⁴⁵ Most recently, Ciabrelli et al. reported that catalytic-dead CBP/Gcn5 recapitulates the function of the WT protein in driving zygotic genome activation.²⁸ Our finding, that BRD4-dependent transcription has no requirement for bromodomain-mediated interaction with histone acetylation, may offer an explanation. H3K27ac may be better considered as an active transcription marker that reflects gene expression status rather than as a determinant for transcription or enhancer activity. The advantage for the cell to dispense with any requirement for histone acetylation would be that during conditions such as cell division and differentiation, rapid and specific gene expression changes could proceed undelayed by the process of histone modification establishment. Indeed, the transcriptional kinetics of up- and down-regulation in response to heat shock are largely independent of the histone modification context at heat-shock-responsive genes.⁴⁶

We did find a handful of genes that are upregulated upon depletion of endogenous BRD4 and for which BRD4 or mutant construct rescue had very different (or opposite) effects compared to those seen at the vast majority of genes. Because these genes were so few, they were not excluded from and did not affect our genome-wide analyses, but they are certainly worth considering separately. Future studies will be needed to address the mechanism of transcriptional activation for these genes. We also observed several genes that were not fully rescued by the bromodomain-less BRD4 mutants, including the gene encoding the important and well-characterized transcription factor MYC. Since the *MYC* locus is known to be regulated by super enhancers, and because super enhancers are bound by Mediator and BRD4 through bromodomains,³² we suspect that the defect in *MYC* rescue could reflect a requirement for the histone-bound layer of BRD4-PTEFb in the maintenance of super enhancer activity. BRD2 has also been shown by our lab and others to be essential for transcriptional regulation,^{47–49} so it will be interesting to investigate whether this function is conserved for bromodomains among different BET family members or if the bromodomains of different BET family members have distinct functional roles.

Limitations of the study

BRD4 mutants were induced prior to auxin depletion of IAA7-tagged, endogenous BRD4, and the result that bromodomain-less BRD4 mutants could rescue the genome-wide Pol II pausing caused by 3 h of endogenous BRD4 depletion, while the same mutants could only rescue transcript levels for a subset of the genes down-regulated by 24 h of depletion, is consistent with potential bromodomain-mediated gene expression regulatory

roles beyond pause release, such as the regulation of transcription initiation^{45,50} and RNA processing.^{30,51} However, endogenous BRD4 activity prior to auxin treatment could potentially establish or poised Pol II machinery in such a way that persistence of such a state after endogenous BRD4 depletion might theoretically enable the full functionality observed upon complementation with the bromodomain-less BRD4. This is a design limitation inherent in the acute depletion setting, which was chosen to avoid the lethality of long-term or total BRD4 depletion in our rescue experiments. Due to the use of pooled lentivirus-infected cells to avoid clonal expression effects, another limitation of the rescue experiments is that the potential contribution of expression level to the differential effects of mutant constructs on the Pol II profile (for example by ΔCTM and BRD4S at the *MYC* locus) is not addressed.

From a conceptual standpoint, our data indicate that either BRD4 or its functional C-terminal fragments can form stable complexes with PTEFb that are capable of CTD phosphorylation to release paused Pol II, regardless of the acetylation status of nearby histones. However, it remains unclear whether a complete loss of all histone acetylation is a survivable condition, because even in the study by Ciabrelli et al., the H3K27ac, H3K9ac, and H3K18ac deposited by CBP/Gcn5 were not simultaneously absent.²⁸ It therefore remains to be determined whether BRD4 could function normally in the total absence of any histone acetylation in living cells. It is entirely possible that acetyl-bound and unbound BRD4-PTEFb populations could act to co-regulate transcription through interdependent mechanisms, but this study does not indicate whether or how this co-regulation might occur.

STAR★METHODS

Detailed methods are provided in the online version of this paper and include the following:

- **KEY RESOURCES TABLE**
- **RESOURCE AVAILABILITY**
 - Lead contact
 - Materials availability
 - Data and code availability
- **EXPERIMENTAL MODEL AND SUBJECT DETAILS**
- **METHOD DETAILS**
 - Drug treatments
 - Generation of degron cell lines
 - Generation and expression of BRD4 mutant constructs
 - Cell growth assay
 - Western blot

Figure 7. The model for transcriptional regulation by a distinct layer of histone acetylation-unbound BRD4-PTEFb complex

Under normal cellular conditions, the majority of BRD4 molecules are associated with chromatin through binding to acetylated histone tails, and the PTEFb complex is recruited by its interaction with the C terminus of BRD4 to form the acetylation-bound “layer” of BRD4-PTEFb. A small portion of the remaining BRD4-PTEFb complex interacts with the Pol II CTD regardless of histone acetylation, forming a critical layer of BRD4-PTEFb that phosphorylates the Ser2 and Ser5 positions of the CTD heptapeptide repeats (panel 1). BRD4 depletion achieved either by auxin in the BRD4 degron cells or dBET6 treatment results in genome-wide Pol II pausing (panel 2). The acetylation-bound BRD4-PTEFb layer is displaced from the chromatin when cells are treated with the bromodomain inhibitor JQ1, but the acetylation-independent layer of BRD4-PTEFb can still function to release Pol II without histone recognition-mediated chromatin association (panel 3). In the absence of acetylation (e.g., H3K27ac, H3K9ac, and H3K18ac deposited by CBP/GCN5²⁸), the acetylation-independent, Pol II-bound BRD4-PTEFb complex retains the ability in releasing Pol II (panel 4).

- GFP IP-MS
- RNA-seq
- ChIP-seq
- QUANTIFICATION AND STATISTICAL ANALYSIS
 - RNA-seq data analysis
 - ChIP-seq analysis

SUPPLEMENTAL INFORMATION

Supplemental information can be found online at <https://doi.org/10.1016/j.molcel.2023.06.032>.

ACKNOWLEDGMENTS

We thank Brianna Monroe for illustrating the findings of this study in the model. We want to thank Emily Rendleman, Sheetal Ganesan, Cassy Philips, and Jacob Zeidner for initial NGS sequencing and Yue He for her participation in the cloning for GFP-tagged ΔBD and C. We also want to thank Drs. Edwin Smith, Marc Morgan, Yuki Aoi and Karen Adelman for in-depth discussions and suggestions for the study. We are grateful for all the current and past Shilatifard lab members for their support. L.W. laboratory is supported by NIH grant R35GM146979. Studies in the Shilatifard lab are supported by generous funding through the Outstanding Investigator Award mechanism by the National Cancer Institute grant R35-CA197569.

AUTHOR CONTRIBUTIONS

B.Z., L.W., and A.S. conceived and designed the experiments. B.Z. carried out the experiments and performed the data analyses. B.C.H. performed the main portion of the NGS library preparation and sequencing. M.I. performed the RNA-seq analysis and reproduced the analyses for ChIP-seq. B.Z. wrote the manuscript, and S.R.G. revised. B.Z., S.R.G., L.W., and A.S. finalized the manuscript.

DECLARATION OF INTERESTS

The authors declare no conflict of interests.

Received: March 24, 2023
 Revised: May 15, 2023
 Accepted: June 26, 2023
 Published: July 12, 2023

REFERENCES

1. Core, L., and Adelman, K. (2019). Promoter-proximal pausing of RNA polymerase II: A nexus of gene regulation. *Genes Dev.* 33, 960–982. <https://doi.org/10.1101/gad.325142.119>.
2. Chen, F.X., Smith, E.R., and Shilatifard, A. (2018). Born to run: Control of transcription elongation by RNA polymerase II. *Nat. Rev. Mol. Cell Biol.* 19, 464–478. <https://doi.org/10.1038/s41580-018-0010-5>.
3. Adelman, K., and Lis, J.T. (2012). Promoter-proximal pausing of RNA polymerase II: emerging roles in metazoans. *Nat. Rev. Genet.* 13, 720–731. <https://doi.org/10.1038/nrg3293>.
4. Price, D.H. (2000). P-TEFb, a Cyclin-Dependent Kinase Controlling Elongation by RNA Polymerase II. *Mol. Cell* 23, 297–305. <https://doi.org/10.1016/j.molcel.2000.06.014>.
5. Peterlin, B.M., and Price, D.H. (2006). Controlling the Elongation Phase of Transcription with P-TEFb. *Mol. Cell* 23, 297–305. <https://doi.org/10.1016/j.molcel.2006.06.014>.
6. Buratowski, S. (2009). Progression through the RNA Polymerase II CTD Cycle. *Mol. Cell* 36, 541–546. <https://doi.org/10.1016/j.molcel.2009.10.019>.
7. Hsin, J.P., and Manley, J.L. (2012). The RNA polymerase II CTD coordinates transcription and RNA processing. *Genes Dev.* 26, 2119–2137. <https://doi.org/10.1101/gad.200303.112>.
8. Lu, X., Zhu, X., Li, Y., Liu, M., Yu, B., Wang, Y., Rao, M., Yang, H., Zhou, K., Wang, Y., et al. (2016). Multiple P-TEFbs cooperatively regulate the release of promoter-proximally paused RNA polymerase II. *Nucleic Acids Res.* 44, 6853–6867. <https://doi.org/10.1093/nar/gkw571>.
9. Lin, C., Smith, E.R., Takahashi, H., Lai, K.C., Martin-Brown, S., Florens, L., Washburn, M.P., Conaway, J.W., Conaway, R.C., and Shilatifard, A. (2010). AFF4, a Component of the ELL/P-TEFb Elongation Complex and a Shared Subunit of MLL Chimeras, Can Link Transcription Elongation to Leukemia. *Mol. Cell* 37, 429–437. <https://doi.org/10.1016/j.molcel.2010.01.026>.
10. Li, Q., Price, J.P., Byers, S.A., Cheng, D., Peng, J., and Price, D.H. (2005). Analysis of the large inactive P-TEFb complex indicates that it contains one 7SK molecule, a dimer of HEXIM1 or HEXIM2, and two P-TEFb molecules containing Cdk9 phosphorylated at threonine 186. *J. Biol. Chem.* 280, 28819–28826. <https://doi.org/10.1074/jbc.M502712200>.
11. Smith, E., Lin, C., and Shilatifard, A. (2011). The super elongation complex (SEC) and MLL in development and disease. *Genes Dev.* 25, 661–672. <https://doi.org/10.1101/gad.2015411>.
12. Zheng, B., Aoi, Y., Shah, A.P., Iwanaszko, M., Das, S., Rendleman, E.J., Zha, D., Khan, N., Smith, E.R., and Shilatifard, A. (2021). Acute perturbation strategies in interrogating RNA polymerase II elongation factor function in gene expression. *Genes Dev.* 35, 273–285. <https://doi.org/10.1101/GAD.346106.120>.
13. Wu, S.Y., and Chiang, C.M. (2007). The double bromodomain-containing chromatin adaptor Brd4 and transcriptional regulation. *J. Biol. Chem.* 282, 13141–13145. <https://doi.org/10.1074/jbc.R700001200>.
14. Gaucher, J., Boussouar, F., Montellier, E., Curtet, S., Buchou, T., Bertrand, S., Hery, P., Jounier, S., Depaux, A., Vitte, A.L., et al. (2012). Bromodomain-dependent stage-specific male genome programming by Brdt. *EMBO J.* 31, 3809–3820. <https://doi.org/10.1038/emboj.2012.233>.
15. Zhang, T., Cooper, S., and Brockdorff, N. (2015). The interplay of histone modifications – writers that read. *EMBO Rep.* 16, 1467–1481. <https://doi.org/10.15252/embr.201540945>.
16. Atlasi, Y., and Stunnenberg, H.G. (2017). The interplay of epigenetic marks during stem cell differentiation and development. *Nat. Rev. Genet.* 18, 643–658. <https://doi.org/10.1038/nrg.2017.57>.
17. Creyghton, M.P., Cheng, A.W., Welstead, G.G., Kooistra, T., Carey, B.W., Steine, E.J., Hanna, J., Lodato, M.A., Frampton, G.M., Sharp, P.A., et al. (2010). Histone H3K27ac separates active from poised enhancers and predicts developmental state. *Proc. Natl. Acad. Sci. USA* 107, 21931–21936. <https://doi.org/10.1073/pnas.1016071107>.
18. Donati, B., Lorenzini, E., and Ciarrocchi, A. (2018). BRD4 and Cancer: Going beyond transcriptional regulation. *Mol. Cancer* 17, 164. <https://doi.org/10.1186/s12943-018-0915-9>.
19. Kanno, T., Kanno, Y., Leroy, G., Campos, E., Sun, H.W., Brooks, S.R., Vahedi, G., Heightman, T.D., Garcia, B.A., Reinberg, D., et al. (2014). BRD4 assists elongation of both coding and enhancer RNAs by interacting with acetylated histones. *Nat. Struct. Mol. Biol.* 21, 1047–1057. <https://doi.org/10.1038/nsmb.2912>.
20. Shorstova, T., Foulkes, W.D., and Witcher, M. (2021). Achieving clinical success with BET inhibitors as anti-cancer agents. *Br. J. Cancer* 124, 1478–1490. <https://doi.org/10.1038/s41416-021-01321-0>.
21. Winter, G.E., Mayer, A., Buckley, D.L., Erb, M.A., Roderick, J.E., Vittori, S., Reyes, J.M., di Julio, J., Souza, A., Ott, C.J., et al. (2017). BET Bromodomain Proteins Function as Master Transcription Elongation Factors Independent of CDK9 Recruitment. *Mol. Cell* 67, 5–18.e19. <https://doi.org/10.1016/j.molcel.2017.06.004>.
22. Mertz, J.A., Conery, A.R., Bryant, B.M., Sandy, P., Balasubramanian, S., Mele, D.A., Bergeron, L., and Sims, R.J. (2011). Targeting MYC dependence in cancer by inhibiting BET bromodomains. *Proc. Natl. Acad. Sci. USA* 108, 16669–16674. <https://doi.org/10.1073/pnas.1108190108>.
23. Lu, J., Qian, Y., Altieri, M., Dong, H., Wang, J., Raina, K., Hines, J., Winkler, J.D., Crew, A.P., Coleman, K., and Crews, C.M. (2015). Hijacking the

- E3 Ubiquitin Ligase Cereblon to Efficiently Target BRD4. *Chem. Biol.* 22, 755–763. <https://doi.org/10.1016/j.chembiol.2015.05.009>.
24. Winter, G.E., Buckley, D.L., Pault, J., Roberts, J.M., Souza, A., Dhe-Paganon, S., and Bradner, J.E. (2015). Phthalimide conjugation as a strategy for *in vivo* target protein degradation. *Science* 348, 1376–1381. <https://doi.org/10.1126/science.aab1433>.
 25. Wang, Z., Chivu, A.G., Choate, L.A., Rice, E.J., Miller, D.C., Chu, T., Chou, S.P., Kingsley, N.B., Petersen, J.L., Finno, C.J., et al. (2022). Prediction of histone post-translational modification patterns based on nascent transcription data. *Nat. Genet.* 54, 295–305. <https://doi.org/10.1038/s41588-022-01026-x>.
 26. Sankar, A., Mohammad, F., Sundaramurthy, A.K., Wang, H., Lerdrup, M., Tatar, T., and Helin, K. (2022). Histone editing elucidates the functional roles of H3K27 methylation and acetylation in mammals. *Nat. Genet.* 54, 754–760. <https://doi.org/10.1038/s41588-022-01091-2>.
 27. Zhang, T., Zhang, Z., Dong, Q., Xiong, J., and Zhu, B. (2020). Histone H3K27 acetylation is dispensable for enhancer activity in mouse embryonic stem cells. *Genome Biol.* 21, 45. <https://doi.org/10.1186/s13059-020-01957-w>.
 28. Ciabrelli, F., Rabbani, L., Cardamone, F., Zenk, F., Löser, E., Schächtle, M.A., Mazina, M., Loubiere, V., and Iovino, N. (2023). CBP and Gcn5 drive zygotic genome activation independently of their catalytic activity. *Sci. Adv.* 9, eadf2687. <https://doi.org/10.1126/sciadv.adf2687>.
 29. Muhar, M., Ebert, A., Neumann, T., Umkehrer, C., Jude, J., Wieshofer, C., Rescheneder, P., Lipp, J.J., Herzog, V.A., Reichholz, B., et al. SLAM-seq defines direct gene-regulatory functions of the BRD4-MYC axis. *Science*, 360(6390), pp.800-805
 30. Arnold, M., Bressin, A., Jasnovidova, O., Meierhofer, D., and Mayer, A. (2021). A BRD4-mediated elongation control point primes transcribing RNA polymerase II for 3'-processing and termination. *Mol. Cell* 81, 3589–3603.e13. <https://doi.org/10.1016/j.molcel.2021.06.026>.
 31. Li, S., Prasanna, X., Salo, V.T., Vattulainen, I., and Ikonen, E. (2019). An efficient auxin-inducible degron system with low basal degradation in human cells. *Nat. Methods* 16, 866–869. <https://doi.org/10.1038/s41592-019-0512-x>.
 32. Lovén, J., Hoke, H.A., Lin, C.Y., Lau, A., Orlando, D.A., Vakoc, C.R., Bradner, J.E., Lee, T.I., and Young, R.A. (2013). Selective inhibition of tumor oncogenes by disruption of super-enhancers. *Cell* 153, 320–334. <https://doi.org/10.1016/j.cell.2013.03.036>.
 33. Itzen, F., Greifenberg, A.K., Bösken, C.A., and Geyer, M. (2014). Brd4 activates P-TEFb for RNA polymerase II CTD phosphorylation. *Nucleic Acids Res.* 42, 7577–7590. <https://doi.org/10.1093/nar/gku449>.
 34. Jang, M.K., Mochizuki, K., Zhou, M., Jeong, H.S., Brady, J.N., and Ozato, K. (2005). The bromodomain protein Brd4 is a positive regulatory component of P-TEFb and stimulates RNA polymerase II-dependent transcription. *Mol. Cell* 19, 523–534. <https://doi.org/10.1016/j.molcel.2005.06.027>.
 35. Phatnani, H.P., and Greenleaf, A.L. (2006). Phosphorylation and functions of the RNA polymerase II CTD. *Genes Dev.* 20, 2922–2936. <https://doi.org/10.1101/gad.147700.6>.
 36. Yang, Z., He, N., and Zhou, Q. (2008). Brd4 Recruits P-TEFb to Chromosomes at Late Mitosis To Promote G 1 Gene Expression and Cell Cycle Progression. *Mol. Cell Biol.* 28, 967–976. <https://doi.org/10.1128/mcb.01020-07>.
 37. Tahirov, T.H., Babayeva, N.D., Varzavand, K., Cooper, J.J., Sedore, S.C., and Price, D.H. (2010). Crystal structure of HIV-1 Tat complexed with human P-TEFb. *Nature* 465, 747–751. <https://doi.org/10.1038/nature09131>.
 38. Pettersen, E.F., Goddard, T.D., Huang, C.C., Meng, E.C., Couch, G.S., Croll, T.I., Morris, J.H., and Ferrin, T.E. (2021). UCSF ChimeraX: Structure visualization for researchers, educators, and developers. *Protein Sci.* 30, 70–82. <https://doi.org/10.1002/pro.3943>.
 39. Shu, S., Lin, C.Y., He, H.H., Witwicki, R.M., Tabassum, D.P., Roberts, J.M., Janiszewska, M., Huh, S.J., Liang, Y., Ryan, J., et al. (2016). Response and resistance to BET bromodomain inhibitors in triple-negative breast cancer. *Nature* 529, 413–417. <https://doi.org/10.1038/nature16508>.
 40. Fong, C.Y., Gilan, O., Lam, E.Y.N., Rubin, A.F., Ftouni, S., Tyler, D., Stanley, K., Sinha, D., Yeh, P., Morison, J., et al. (2015). BET inhibitor resistance emerges from leukaemia stem cells. *Nature* 525, 538–542. <https://doi.org/10.1038/nature14888>.
 41. Rathert, P., Roth, M., Neumann, T., Muerdter, F., Roe, J.S., Muhar, M., Deswal, S., Cerny-Reiterer, S., Peter, B., Jude, J., et al. (2015). Transcriptional plasticity promotes primary and acquired resistance to BET inhibition. *Nature* 525, 543–547. <https://doi.org/10.1038/nature14898>.
 42. Calder, J., Nagelberg, A., Luu, J., Lu, D., and Lockwood, W.W. (2021). Resistance to BET inhibitors in lung adenocarcinoma is mediated by casein kinase phosphorylation of BRD4. *Oncogenesis* 10, 27. <https://doi.org/10.1038/s41389-021-00316-z>.
 43. Sun, Y., Zhang, Z., Zhang, K., Liu, Y., Shen, P., Cai, M., Jia, C., Wang, W., Gu, Z., Ma, P., et al. (2021). Epigenetic heterogeneity promotes acquired resistance to BET bromodomain inhibition in ovarian cancer. *American Journal of Cancer Research* 11, 3021.
 44. Andrieu, G., Belkina, A.C., and Denis, G.V. (2016). Clinical trials for BET inhibitors run ahead of the science. *Drug Discov. Today Technol.* 19, 45–50. <https://doi.org/10.1016/j.ddtec.2016.06.004>.
 45. Narita, T., Ito, S., Higashijima, Y., Chu, W.K., Neumann, K., Walter, J., Satpathy, S., Liebner, T., Hamilton, W.B., Maskey, E., et al. (2021). Enhancers are activated by p300/CBP activity-dependent PIC assembly, RNAPII recruitment, and pause release. *Mol. Cell* 81, 2166–2182.e6. <https://doi.org/10.1016/j.molcel.2021.03.008>.
 46. Mahat, D.B., Salamanca, H.H., Duarte, F.M., Danko, C.G., and Lis, J.T. (2016). Mammalian Heat Shock Response and Mechanisms Underlying Its Genome-wide Transcriptional Regulation. *Mol. Cell* 62, 63–78. <https://doi.org/10.1016/j.molcel.2016.02.025>.
 47. Cheung, K.L., Zhang, F., Jaganathan, A., Sharma, R., Zhang, Q., Konuma, T., Shen, T., Lee, J.Y., Ren, C., Chen, C.H., et al. (2017). Distinct Roles of Brd2 and Brd4 in Potentiating the Transcriptional Program for Th17 Cell Differentiation. *Mol. Cell* 65, 1068–1080.e5. <https://doi.org/10.1016/j.molcel.2016.12.022>.
 48. Wang, C., Xu, Q., Zhang, X., Day, D.S., Abraham, B.J., Lun, K., Chen, L., Huang, J., and Ji, X. (2022). BRD2 interconnects with BRD3 to facilitate Pol II transcription initiation and elongation to prime promoters for cell differentiation. *Cell. Mol. Life Sci.* 79, 338. <https://doi.org/10.1007/s00018-022-04349-4>.
 49. Hsu, S.C., Gilgenast, T.G., Bartman, C.R., Edwards, C.R., Stonestrom, A.J., Huang, P., Emerson, D.J., Evans, P., Werner, M.T., Keller, C.A., et al. (2017). The BET Protein BRD2 Cooperates with CTCF to Enforce Transcriptional and Architectural Boundaries. *Mol. Cell* 66, 102–116.e7. <https://doi.org/10.1016/j.molcel.2017.02.027>.
 50. Donczew, R., and Hahn, S. (2021). BET family members Bdf1/2 modulate global transcription initiation and elongation in *Saccharomyces cerevisiae*. *Elife* 10, e69619. <https://doi.org/10.7554/eLife.69619>.
 51. Hussong, M., Kaehler, C., Kerick, M., Grimm, C., Franz, A., Timmermann, B., Welzel, F., Isensee, J., Hucho, T., Krobtsch, S., and Schweiger, M.R. (2017). The bromodomain protein BRD4 regulates splicing during heat shock. *Nucleic Acids Res.* 45, 382–394. <https://doi.org/10.1093/nar/gkw729>.
 52. Langmead, B., Trapnell, C., Pop, M., and Salzberg, S.L. (2009). Ultrafast and memory-efficient alignment of short DNA sequences to the human genome. *Genome Biol.* 10, R25. <https://doi.org/10.1186/gb-2009-10-3-r25>.
 53. Trapnell, C., Pachter, L., and Salzberg, S.L. (2009). TopHat: discovering splice junctions with RNA-Seq. *Bioinformatics* 25, 1105–1111. <https://doi.org/10.1093/bioinformatics/btp120>.

54. Love, M.I., Huber, W., and Anders, S. (2014). Moderated estimation of fold change and dispersion for RNA-seq data with DESeq2. *Genome Biol.* 15, 550. <https://doi.org/10.1186/s13059-014-0550-8>.
55. Ramírez, F., Ryan, D.P., Grüning, B., Bhardwaj, V., Kilpert, F., Richter, A.S., Heyne, S., Dündar, F., and Manke, T. (2016). deepTools2: a next generation web server for deep-sequencing data analysis. *Nucleic Acids Res.* 44, W160–W165. <https://doi.org/10.1093/NAR/GKW257>.
56. Liao, Y., Smyth, G.K., and Shi, W. (2014). FeatureCounts: An efficient general purpose program for assigning sequence reads to genomic features. *Bioinformatics* 30, 923–930. <https://doi.org/10.1093/bioinformatics/btt656>.
57. Risso, D., Ngai, J., Speed, T.P., and Dudoit, S. (2014). Normalization of RNA-seq data using factor analysis of control genes or samples. *Nat. Biotechnol.* 32, 896–902. <https://doi.org/10.1038/nbt.2931>.
58. Langmead, B., and Salzberg, S.L. (2012). Fast gapped-read alignment with Bowtie 2. *Nat. Methods* 9, 357–359. <https://doi.org/10.1038/nmeth.1923>.
59. Aoi, Y., Shah, A.P., Ganesan, S., Soliman, S.H.A., Cho, B.K., Goo, Y.A., Kelleher, N.L., and Shilatifard, A. (2022). SPT6 functions in transcriptional pause/release via PAF1C recruitment. *Mol. Cell* 82, 3412–3423.e5. <https://doi.org/10.1016/j.molcel.2022.06.037>.

STAR★METHODS

KEY RESOURCES TABLE

REAGENT or RESOURCE	SOURCE	IDENTIFIER
Antibodies		
BRD4 (for WB)	Cell Signaling Technology	Cat#13440; RRID:AB_2687578
β-Actin (for WB)	Cell Signaling Technology	Cat#3700; RRID:AB_2242334
V5-Tag (for WB)	Cell Signaling Technology	Cat#13202; RRID:AB_2687461
HA-Tag (for WB)	Cell Signaling Technology	Cat#3724S; RRID:AB_1549585
CDK9 (for WB)	Cell Signaling Technology	Cat#2316; RRID:AB_2291505
Cyclin T1 (for WB and ChIP)	Cell Signaling Technology	Cat#81464; RRID:AB_2799973
Tubulin (for WB)	Developmental Studies Hybridoma Bank	Cat#E7; RRID:AB_528499
FLAG (for WB)	Millipore Sigma	Cat#F1804; RRID:AB_262044
GFP (for WB)	Santa Cruz Biotechnology	Cat#sc-9996; RRID:AB_627695
H3 (for WB)	This study	NA
BRDT (for WB)	This study	NA
Rpb1 (for ChIP)	Cell Signaling Technology	Cat#14958S; RRID:AB_2687876
Ser2p (for ChIP)	Active Motif	Cat#61984; RRID:AB_2687450
CDK9 (for ChIP)	Santa Cruz Biotechnology	Cat#sc-13130 X; RRID:AB_627245
GFP (for ChIP)	Developmental Studies Hybridoma Bank	Cat#GFP-G1; RRID:AB_2619561
GFP (for ChIP)	Developmental Studies Hybridoma Bank	Cat#GFP-12A6; RRID:AB_2617417
GFP (for ChIP)	Developmental Studies Hybridoma Bank	Cat#GFP-12E6; RRID:AB_2617418
GFP (for ChIP)	Developmental Studies Hybridoma Bank	Cat#GFP-8H11; RRID:AB_2617423
Chemicals, peptides, and recombinant proteins		
Auxin (3-Indole-acetic acid sodium salt)	Abcam	Cat#ab146403
JQ1	Tocris	Cat#4499
dBET6	Selleckchem	Cat#S876202
NVP-2	MedChemExpress	Cat#HY-12214A
THAL-SNS-032 (dCDK9)	MedChemExpress	Cat#HY-123937
Doxycycline	Stem Cell Technologies	Cat#72742
Benzonase	Millipore Sigma	Cat#E1014
Dynabeads Protein G	Invitrogen	Cat#10004D
ChromoTek GFP-Trap Magnetic Agarose	Proteintech	Cat#gtma
Deposited data		
Genomics data	This study	GSE232869
Experimental models: Cell lines		
DLD-1	ATCC	Cat#CCL-221
NCI-H2009	ATCC	Cat#CRL-5911
Mouse embryonic fibroblasts	STEMCELL Technologies	Cat#00325
BRD4-IAA7 DLD1 #G3/D4	This study	NA
Recombinant DNA		
Cas9 plasmid for BRD4-IAA7 (sgRNA: CACCGAATCTTT TCTGAGCGCACCT)	Zheng et al., 2021 ¹²	NA

(Continued on next page)

Continued

REAGENT or RESOURCE	SOURCE	IDENTIFIER
Cas9 plasmid for BRD4-IAA7 (sgRNA: CACCGATCAAAGTCAGAACCCACCT)	Zheng et al., 2021 ¹²	NA
BRD4-IAA7-Neo donor plasmid	This study	pBZ14
BRD4-IAA7-Hygro donor plasmid	This study	pBZ15
Lenti-TetON-Sox2	Addgene	Cat#110280
p6344 pcDNA4-TO-HA-Brd4FL	Addgene	Cat#31351
pFlag-CMV2-Brd4 del ET	Addgene	Cat#21938
pTet-On-sNLS-3xFlag-EGFP-UBC-rtTeR-IRES-BSD	This study	pBZ113
pTet-On-sNLS-3xFlag-BRD4-FL-UBC-rtTeR-IRES-BSD	This study	pBZ111
pTet-On-sNLS-3xFlag-BRD4-ΔBD-UBC-rtTeR-IRES-BSD	This study	pBZ160
pTet-On-sNLS-3xFlag-BRD4-ΔET-UBC-rtTeR-IRES-BSD	This study	pBZ136
pTet-On-sNLS-3xFlag-BRD4-ΔCTM-UBC-rtTeR-IRES-BSD	This study	pBZ158
pTet-On-sNLS-3xFlag-BRD4S-UBC-rtTeR-IRES-BSD	This study	pBZ137
pTet-On-sNLS-3xFlag-BRD4-ΔN-UBC-rtTeR-IRES-BSD	This study	pBZ176
pTet-On-sNLS-3xFlag-BRD4-Cm-UBC-rtTeR-IRES-BSD	This study	C1
pTet-On-sNLS-3xFlag-BRD4-C-UBC-rtTeR-IRES-BSD	This study	C2
pTet-On-sNLS-3xFlag-BRD4-Cs-UBC-rtTeR-IRES-BSD	This study	C3
pTet-On-sNLS-GFP-UBC-rtTeR-IRES-BSD (Vector)	This study	MS1
pTet-On-sNLS-GFP-BRD4-FL-UBC-rtTeR-IRES-BSD	This study	MS0
pTet-On-sNLS-GFP-BRD4-CTM-UBC-rtTeR-IRES-BSD	This study	MS2
pTet-On-sNLS-GFP-BRD4-CsΔCTM-UBC-rtTeR-IRES-BSD	This study	MS3
pTet-On-sNLS-GFP-BRD4-Cs-UBC-rtTeR-IRES-BSD	This study	MS4
pTet-On-sNLS-GFP-BRD4-C-UBC-rtTeR-IRES-BSD	This study	MS6
pTet-On-sNLS-GFP-BRD4-FL-ΔBD-UBC-rtTeR-IRES-BSD	This study	MS7
pTet-On-sNLS-GFP-BRD4-FL-ΔCd-UBC-rtTeR-IRES-BSD	This study	pBZ196
pTet-On-sNLS-GFP-BRD4-FL-ΔCdp-UBC-rtTeR-IRES-BSD	This study	pBZ197
Software and algorithms		
bowtie 2.2.6.0	Langmead et al., 2009 ⁵²	NA
TopHat 2.1.0	Trapnell et al., 2009 ⁵³	NA
DESeq2	Love et al., 2014 ⁵⁴	NA
deepTools 3.1.1	Ramírez et al., 2016 ⁵⁵	NA
featureCounts 2.0.1	Liao et al., 2014 ⁵⁶	NA
AlphaFold integrated in ChimeraX	Pettersen et al., 2021 ³⁸	NA

RESOURCE AVAILABILITY**Lead contact**

Further information and requests for reagents should be directed to and will be fulfilled by the lead contact, Ali Shilatifard (ash@northwestern.edu).

Materials availability

Unique reagents generated in this study are available from the [lead contact](#) without restriction.

Data and code availability

- All genomic data generated in this study have been deposited to GEO under the accession number GSE232869 and are publicly available as of the date of publication. Accession number is listed in the [key resources table](#).
- This paper does not report original code.
- Any additional information required to reanalyze the data reported in this paper is available from the [lead contact](#) upon request.

EXPERIMENTAL MODEL AND SUBJECT DETAILS

DLD1 (CCL-221) and NCIH2009 (CRL-5911) human cells were purchased from ATCC.

BRD4-IAA7 DLD1 degron cells were generated as described in the following section. DLD1 and NCIH2009 cell lines were cultured in DMEM (Corning, #10013CV) and PRMI 1640 (ThermoFisher, #A1049101) respectively, supplemented with 10% FBS (Sigma-Aldrich, #F2442), 1% Glutmax (Gibco, #35050061), and 1% PS (Gibco, #15140122), in 37°C incubator with 5% CO₂.

METHOD DETAILS

Drug treatments

Auxin (#ab146403) was purchased from abcam. Doxycycline (#72742) was obtained from Stem Cell Technologies. JQ1 (#4499) was purchased from Tocris. dBET6 (#S876202) was purchased from Selleckchem. NVP-2 (#HY-12214A) and dCDK9 (#HY-123937) were purchased from MedChemExpress.

Generation of degron cell lines

BRD4-IAA7 DLD1 degron cells were generated similarly to previously described.¹² Specifically, PX330 (Addgene, #42230) altered with the insertion of sgRNA (#1 AATCTTTCTGAGCGCACCT, or #2 ATCAAAGTCAGAACGCCACCT) targeting the stop codon area of the BRD4 genomic locus was co-transfected with a donor plasmid using the Lipofectamine 3000 Transfection Reagent (Invitrogen, #L3000001) to trigger donor integration at the target site via homologous recombination repair. The donor plasmid, which we designed to integrate the IAA7 tag after the final BRD4 exon and introduce the F box protein AtAFB2 under the EFla promoter, was made using the pBlueScript II SK (+) backbone and synthesized gBlocks for the IAA7-AtAFB2 pair and antibiotic selection marker. Upon transfection, DLD1 cells were selected for colony formation in the presence of either Geneticin (Gibco, #10131027) or hygromycin B (Invitrogen, #10687010) for 2 weeks. Single clone colonies were picked and verified by PCR and western blot analysis.

Generation and expression of BRD4 mutant constructs

TetOn lentiviral vector (#110280), BRD4-FL cDNA (#31351), and BRD4-ΔET cDNA (#21938) were obtained from Addgene. The BRD4S mutant was generated from TetOn-FLAG-BRD4-FL using the Q5 Site-Directed Mutagenesis Kit (NEB, #E0554S). All other BRD4 mutant constructs were generated via NEBuilder HiFi DNA assembly reaction (NEB, #E2621S) with synthesized gBlocks (IDT and Twist Biosciences). TetOn-BRD4 lentiviral constructs were amplified by transformation of stable competent *E. coli* (NEB, #C3040H). All BRD4 plasmid insertions were verified by Sanger sequencing (ACGT). Lentivirus for transducing mammalian expression of the BRD4 mutants was generated by co-transfecting BRD4 mutant expressing plasmids with pspax2/pmd2.g lentiviral packaging plasmids in 293T cells in 6-well format. Lentivirus was collected and filtered for infection of BRD4-IAA7 DLD1 cells in 6-well plates. Infected cells were selected with Blasticidin (Gibco, #A1113903) for two weeks. BRD4 mutant expression was achieved by adding 50nM Dox into the medium and incubating for 48h.

Cell growth assay

0.1 million FLAG-tagged mutants transfected and Blasticidin selected BRD4-IAA7 cells were seeded in 12-well plates on Day 0. Dox was added to induce the mutants' expression. On Day 2, changed to fresh medium and added Dox to maintain the mutants' expression while adding auxin to deplete the endogenous BRD4. On day 4, changed to fresh medium and maintained with Dox and auxin. On Day 2, 4 and 6, when collected, each plate was fixed with 4% paraformaldehyde solution (Fisher Scientific, #50-980-495) in PBS for 20 min at room temperature under shaking. Then plates were washed with tap water for 3 times and dried overnight. Violet solution (Millipore Sigma, #HT90132) was used to stain the fixed cells.

Western blot

Whole cell lysates for western blot were prepared by directly lysing the cells with Laemmli sample buffer (Bio-Rad, #1610747) and boiling for 10 min. BRD4 (#13440), β-Actin (#3700), V5-Tag (#13202), HA-Tag (#3724S), CDK9 (#2316), and Cyclin T1 (#81464) antibodies were purchased from Cell Signaling Technology. Tubulin (#E7) antibody was obtained from Developmental Studies Hybridoma Bank (DSHB). FLAG antibody (#F1804) was obtained from Millipore Sigma. GFP Antibody (#sc-9996) was purchased from Santa Cruz Biotechnology. H3 and BRDT antibodies were generated in-house. Western blot quantification was carried out with the ImageLab from Bio-Rad.

GFP IP-MS

To prepare the GFP IP-MS samples, cells were released with trypsin and washed with PBS before incubation in cold Buffer A (10mM HEPES pH 7.9, 10mM KCl, 1.5mM MgCl₂, DTT (Thermo Scientific, #A39255), Protease inhibitor (Thermo Scientific, #PIA32963), and Phosphatase inhibitor (Thermo Scientific, #PIA32957)) for nuclear isolation. Nuclear pellets were lysed by the addition of cold Triton X-100 lysis buffer (50mM Tris HCl, pH 8.0, 150mM NaCl, 1.5mM MgCl₂, 10% Glycerol, 0.5% Triton X-100, DTT, Benzonase, Protease inhibitor, and Phosphatase inhibitor) followed by rotation for 45min and centrifugation at 20,000g for 15 min (all at 4°C.) The supernatant was incubated with ChromoTek GFP-Trap magnetic beads (Proteintech, #gtma) for > 4h at 4°C for immunoprecipitation, then

beads were washed 5x with cold Triton X-100 lysis buffer and 1x with cold Triton X-100 wash buffer (50mM Tris HCl, pH 8.0, 150mM NaCl, 1.5mM MgCl₂, 1.5mM EDTA, DTT). Glycine 2.5M pH 2.0 was used to elute the immunoprecipitated proteins and Tris buffer pH > 10 was used to neutralize the eluate at RT. Neutralized eluate was snap frozen for MS or mixed with Laemmli sample buffer and boiled for 5 min for western blot. MS was carried out by the Proteomics Core Facility at the University of Arkansas for Medical Sciences.

RNA-seq

Total RNAs from 6-well plate were extracted using the RNeasy mini kit from Qiagen (Qiagen, #74106). mRNAs were enriched using a NEBNext poly(A) mRNA magnetic isolation module (NEB, #E7490L). RNA libraries were prepared using NEBNext Ultra II Directional RNA library preparation kit (NEB, #E7760L) and sequenced on the Illumina NovaSeq 6000.

ChIP-seq

DLD1 cells were crosslinked with 15mL 1% PFA (ThermoFisher, #28908) in PBS on 15cm plates for 10 min at RT and quenched by the addition of 2mL 2.5M glycine followed by shaking for 5 min. Crosslinked cells were collected by scraping. Chromatin sonication was performed for 10 min using a Covaris E200 set to 10% duty factor, 200 cycles per burst, and 140 peak intensity power. For endogenous protein ChIP, 10–20% of mouse embryonic fibroblasts (MEF) chromatin (prepared the same way as in DLD1 cells) was added to each sample as a spike-in control. For overexpressed protein ChIP, such as GFP-ChIP, 20ng spike-in chromatin (Active Motif, #53083) and 2ug spike-in antibody (Active Motif, #61686) were added to each sample. Immunoprecipitation was carried out at 4°C overnight using 5ul of Rpb1 (Cell Signaling Technology, #D8L4Y), 5ul of Ser2p (Active Motif, #61984), 10ul of CCNT1 (Cell Signaling Technology, #81464), 10ul of CDK9 (Santa Cruz Biotechnology, #sc-13130 X) antibodies, or 200ul of a cocktail consisting of 50ul of each GFP antibody (DSHB, #GFP-G1, #GFP-12A6, #GFP-12E6, #GFP-8H11). Immune complexes were enriched with Protein G-coupled Dynabeads (Invitrogen, #10004D) at 4°C for ≥ 4h, and incubated with proteinase K (Roche, #3115828001) to reverse crosslink at 65°C overnight. Eluted DNA was purified with the QIAquick PCR Purification Kit (Qiagen, #28106), and libraries were prepared using the KAPA HTP library preparation kit (Roche, #07961901001) for sequencing on the NovaSeq 6000.

QUANTIFICATION AND STATISTICAL ANALYSIS

RNA-seq data analysis

Reads were aligned to the human genome (hg38) using Bowtie version 2.2.6.0⁵² and a TopHat run (v2.1.0).⁵³ RNA-Seq read counts were corrected for technical differences and normalized between samples with R package RUVseq⁵⁷ using upper-quartile (UQ) approach. Differential gene expression analysis was performed with DESeq2⁵⁴ with significance thresholds of adj.p < 0.05 and |log₂FC|>0.585.

ChIP-seq analysis

Reads were aligned to hg38 with bowtie 1/2.⁵⁸ Genes (N = 6,481) with pausing site and TES annotation were obtained from a previously published study.⁵⁹ Promoter regions were designated as spanning from 100bp upstream to 300bp downstream of the pausing site. Gene body regions were designated as spanning from 300bp downstream of the pausing site to the TES. FeatureCounts 2.0.1⁵⁶ was used to calculate the total mapped reads from Pol II ChIP-seq at promoters and within gene bodies. PRR is calculated as the ratio of Pol II signal density within the gene body to Pol II signal density at the promoter. BamCoverage in deeptools 3.1.1⁵⁵ was used to extend ChIP-seq reads to 150bp. Log₂FC of ChIP-seq was calculated using bigwigCompare in deeptools with the following nondefault options: binSize 10, pseudocount 0.1. Heatmaps and metagene plots were also generated in deeptools. ECDFs and boxplots/scatterplots for the log₂PRR and MS were generated using R. Tracks were visualized in igv 2.13.2 (Broad Institute).